UNIVERSITY OF OSLO

Master's thesis

Gravitational waves from topological defects

Signatures of late-time first-order phase transitions

Nanna Bryne

Computational Science: Astrophysics
60 ECTS study points

Institute of Theoretical Astrophysics, Department of Physics
Faculty of Mathematics and Natural Sciences

Autumn 2024

Nanna Bryne

Gravitational waves from topological defects

Signatures of late-time first-order phase transitions

Supervisor:
David Fonseca Mota

Contents

Notation v

1

1 Introduction 5
1.1 Preliminaries 6
1.1.1 Field theory 6
1.1.2 Expanding universe: standard cosmology 7
1.1.3 Method of Green's functions 7

I Background **9**

2 General Relativity 11
2.1 Differential geometry 11
2.1.1 Hypersurfaces 11
2.1.2 Conformal geometry 11
2.2 Einstein's equation 12
2.3 Standard model of cosmology 13
2.3.1 Cosmological perturbation theory 14
2.3.2 Hubble trouble 14
2.4 Linearised gravity; tensor sector 15
2.4.1 Gravitational waves in an expanding universe 15
2.4.2 Polarisation of tensor modes / TITLE (Effect on test particles) . 16
3 TITLE (Kinks in Cosmology) 17
3.1 TITLE (Topological defects) 17
3.1.1 Example: (stationary) $\mathbb{Z}_2$ kinks 18
3.1.2 TITLE (Domain walls) 19
3.1.3 Defect formation 19
3.2 TITLE (Quintessence) 20
3.2.1 General framework 20
3.2.2 Asymmetron model 21

II Methodology **23**

4 Imperfect Defects 25
4.1 TITLE (Kink dynamics / General formula) 25
4.1.1 Linearised perturbations 26
4.1.2 Energy and momentum 27

4.2 Dynamics of planar domain walls in expanding universe 27
4.2.1 Time-dependent surface tension 28
4.3 TITLE (Symmetron domain walls) 29
4.3.1 Solution in matter-dominated universe 29
4.3.2 TITLE (Review) 31
4.4 Generation of gravitational waves 32
4.4.1 TITLE (Dynamics of gravitational waves in expanding universe) 33
4.4.2 Fourier space stress–energy tensor 33
4.4.3 Examples 35
5 TITLE (Cosmic Phase Transition) 39
5.1 $\mathbb{Z}_2$ symmetry break 39
5.1.1 Quasistatic limit 40
5.1.2 Asymptotic limit 40
5.2 Dynamic modelling 41
5.3 `gwasevolution` (On the lattice?) 41
5.3.1 Periodic boundaries 41
5.3.2 Initial configuration 41
5.3.3 Discrete Fourier space 43
5.3.4 TITLE (Options/parameters) 44
5.4 Simulation setups 45
5.4.1 Catalogue 45

III Findings **47**

6 TITLE (Toy Model Trials) 49
6.1 Background evolution / Symmetron field 49
6.1.1 TITLE (Discussion) 50
6.2 Domain wall dynamics 50
6.2.1 Adjusting the equation of motion 52
6.2.2 TITLE (Discussion) 52
6.3 TITLE (Gravitational waves) 53
6.3.1 TITLE (About the comparison) 54
6.3.2 Changing the input to the expression 54
7 TITLE (Ifs, buts and maybes) 55
7.1 Limitations and possibilities 55
7.2 Superpositions 55
7.3 Improvements 56
7.4 Simulative experiments within reach 56
8 Conclusion and Outlook 57
8.1 Applications 57
8.2 Future work 57

59

Bibliography 62
A Derivations 63
A.1 Linearised gravity 63
A.2 Variation of stress–energy tensor 63
A.3 Fourier space stress–energy tensor: sinusoidal 63

B TITLE (Stable Symmetron) 65
B.1 Field initialisation 66
C TITLE (Cylinder Functions) 67
C.1 Properties 67

Notation

Constants and units. We use ⌈'natural units'⌋? where $\hbar = c = 1$, where $\hbar$ is the reduced Planck constant and c is the speed of light in vacuum.⌈Planck units? Set $k_B = G_N = 1$?⌋ The Newtonian constant of gravitation G_N is referenced explicitly, and we use Planck units such as the Planck mass $M_{Pl} = (\hbar c/G_N)^{1/2} = G_N^{-1/2} \sim 10^{-8}$ kg.

Tensors. The metric signature $(-,+,+,+)$ is considered, i.e. $\det[g_{\mu\nu}] \equiv |g| < 0$. The Minkowski metric is denoted $\eta_{\mu\nu}$, whereas a general metric is denoted $g_{\mu\nu}$. A four-vector $p^\mu =$

$[\eta_{\mu\nu}] = \mathrm{diag}(-1,1,1,1)$

$f_{,\mu} \equiv \partial_\mu f = \frac{\partial f}{\partial x^\mu}$

Christophel symbols. The Christophel symbols or "connections" are written

$$\Gamma^\rho_{\mu\nu} = \frac{1}{2} g^{\rho\sigma}\left(g_{\mu\sigma,\nu} + g_{\mu\sigma,\nu} - g_{\mu\nu,\sigma}\right) \tag{1}$$

"Lambda tensor." We express the *Lambda tensor*—sometimes called the "projection operator"—that projects onto the TT gauge refer to sec.© as

$$\Lambda_{ij}{}^{kl}(\boldsymbol{n}) = P_i{}^k(\boldsymbol{n}) P_j{}^l(\boldsymbol{n}) - \frac{1}{2} P_{ij}(\boldsymbol{n}) P^{kl}(\boldsymbol{n}); \quad P_{ij}(\boldsymbol{n}) = \delta_{ij} - n_i n_j \tag{2}$$

$\forall\, \boldsymbol{n}$ of unit length; $\boldsymbol{n}^2 = n_1^2 + n_2^2 + n_3^2 = 1$.

Fourier transforms. We use the following convention for the Fourier transform of $f(x)$, $\tilde{f}(k)$, and its inverse, where x and k are Lorentz four-vectors:

$$\begin{aligned} f(x) &= \int \frac{d^4k}{(2\pi)^4}\, \mathrm{e}^{-\mathrm{i}k\cdot x} \tilde{f}(k) \\ \tilde{f}(k) &= \int d^4x\, \mathrm{e}^{\mathrm{i}k\cdot x} f(x) \end{aligned} \tag{3}$$

Here, $k \cdot x = k_\sigma x^\sigma = g_{\rho\sigma} k^\rho x^\sigma$.

Acronyms

CDM	*c*old *d*ark *m*atter	Page 5
CMB	*c*osmic *m*icrowave *b*ackground [radiation]	p. 25
DW	*d*omain *w*all	
eom	*e*quation *o*f *m*otion	
F(L)RW	*F*riedmann(–*L*emaître)–*R*obertson–*W*alker [metric]	
GR	*g*eneral *r*elativity	
GW	*g*ravitational *w*ave	
lhs	*l*eft-*h*and *s*ide	
NG	*N*ambu–*G*oto [action]	
ODE	*o*rdinary *d*ifferential *e*quation	
PDE	*p*artial *d*ifferential *e*quation	
PT	*p*hase *t*ransition	
rhs	*r*ight-*h*and *s*ide	
SE	*s*tress–*e*nergy [tensor]	
(S)SB	(*s*pontaneous) *s*ymmetry *b*reaking	
TT	*t*ransverse-*t*raceless [gauge]	
ΛCDM	Lambda (Λ) *c*old *d*ark *m*atter model; standard model of cosmology	

Nomenclature

In the table below is listed the most frequently used symbols in this paper, for reference.

Table 1: helo

Symbol	Referent	SI-value or definition
Natural constants		
G_{N}	Newtonian constant of gravitation	1.2 kg
k_{B}	Boltzmann's constant	1.2 K
Fiducial quantities		
h_0	Reduced Hubble constant	0.67
Subscripts		
Functions and operators		
$\Theta(\xi)$	Heaviside step function	$\begin{cases} 1 & \xi > 0 \\ 0 & \xi < 0 \end{cases}$
$\mathrm{sgn}(\xi)$	Signum function	$2\Theta(\xi) - 1$
$\delta^{(n)}\xi$	Dirac-Delta function of $\xi \in \mathbb{R}^n$, $n \in \mathbb{N}$.	
$\delta^{\mu\nu}$	Kronecker delta.	
Mathematical groups		
$\mathsf{Conf}(\mathscr{M})$	The conformal group of the manifold $\mathscr{M}$.	
hh	...	...
Physical quantities		
a	Scale factor.	
$g_{\mu\nu}$	Metric tensor.	
τ	Conformal time.	
s	...	...

Some title		Some title	
Cosmology ⌜SORT!⌟		⋮	⋮
a	Scale factor.	⋮	⋮
$\mathcal{H}$	Conformal Hubble factor $\dot{a}/a$.	⋮	⋮
$\mathfrak{z}$	Cosmic redshift.	⋮	⋮
τ	Conformal time.	υ	Time variable $(a_*/a)^{3\alpha}$.
α	Exponent blah blah [...]	s	Dimensionless conformal time τ/τ_*
$g_{\mu\nu}$	Metric tensor, FLRW.	*Subscripts*	
$\boldsymbol{x}$	Comoving coordinate (x, y, z).	m	Normal matter.
$\boldsymbol{k}$	Comoving wavevector (k_x, k_y, k_z).	0	Today ($a_0 = 1$ is the scale factor today).
$\mathscr{M}$	Riemannian manifold.	$*$	Time of phase transition.
$\mathbb{Z}_n$	Symmetry XXX.		
⋮	⋮		

Table 2: Variables blah blah [...]

DRAFT

Writing Tools

This is a comment.
This needs spelling check.? Perhaps this?
Rephrase this.
Awkward wording.
Needs double-checking.?
This is in need of citation or reference to a section.© (With a comment.)
blah blah [. . .] (Phantom text.)

PHANTOM PARAGRAPH: THIS IS A PHANTOM PARAGRAPH, MAYBE WITH SOME KEYWORDS.

- This is a note.
- This is another note.
  - This is a related note.

This is very important.

This text is highlighted.

Statement. [←That needs to be shown or proven.]

TITLE (Temporary title.)

¿ *Question* Why? ?

Pensive: for thoughts and jokes.

(chapter) Title Case

Lorem ipsum...

(section) Sentence case

Lorem ipsum...

(subsection) Sentence case

Lorem ipsum...

(paragraph) Sentence case with punctuation. Lorem ipsum...
Below, we describe some phenomena or whatever.

Gravitational waves are called that or GWs, tensor perturbations, ... pdsfovnsoz avoszjasvo aoc awvn anvo pewnfvao noav

Stress–energy tensor is called that or SE tensor(?) ⌜OBS: Hilbert SE tensor = HSE tensor?⌟.

Domain walls are called that or walls, never DWs.

General relativity is called that or GR, Einstein's theory of gravity.

Einstein field equation(s) are called that or EFE(s).

Equation(s) of motion are called that or eom(s).

Chapter 1

Introduction

- GOALS:
  - Gather framework about GWs from DWs
  - Remove the need for very expensive N-body simulations with (semi-)analytical predictions
  - Extract as much information as possible from the NANOgrav spectra thingy
- WHY RELEVANT:
  - NANOgrav data wihoo
  - Simulations in this regard are hugely expensive, and will not allow us to constrain the parameters of a model

The thesis is divided into three parts. Part I presents the relevant background theory, including concepts from differential geometry to topological defects. In Part II (pre-sims / a priori) we describe how the framework was designed and the way it is to be tested in simulations. Finally, in Part III (post-sims), we present the results from simulations and calculations, with comparisons and discussions. Prior to all of this, we describe some basic concepts in the coming section.

DRAFT

Final product. We end up with a framework that describes the motion of a small perturbation to the normal coordinate of a planar domain wall in a matter-dominated universe, with possibility for generalisation. The model assumes the symmetron potential, but this is easily changed to another scalar field model with discrete symmetry by changing the surface tension. The equations are tested by comparison to toy scenarios in cosmological simulations. The final part—the resulting tensor perturbations to the metric—has room for improvement, or at least needs to be better tested more thoroughly against simulations. There is no doubt that the signature from such a wall position distortion is detectable *in simulations*, but there are other features of the resulting tensor modes that remain mysterious.

1.1 Preliminaries

It is assumed that the reader is familiar with variational calculus and linear perturbation theory.

⌈In the following, we briefly (re)capture some concepts that are important starting points for the rest of the thesis.⌋

- variational calculus/ varying action
- action
- pert. theory?
- line element
- gauge invariance
- FRW cosmology
- classical field theory

$$G_{\mu\nu} = 8\pi G_{\mathrm{N}} T_{\mu\nu} \tag{1.1}$$

1.1.1 Field theory

We formulate a theory in four-dimensional spacetime ⌈Minkowski⌋ in terms of the Lorentz invariant action

$$S = \int d^4x\, \mathcal{L}(\{\phi_i\}, \{\partial_\mu \phi_i\}), \tag{1.2}$$

with $\mathcal{L}$ being the *Lagrangian density* of the theory, a function of the set of fields $\{\phi_i\}$ and its first derivatives. We will refer to $\mathcal{L}$ simply as the Lagrangian, as is customary when working with fields. For a general (i.e. curved) spacetime, blah blah [...] $\partial_\mu \to \nabla_\mu$ blah blah [...] to construct a Lorentz invariant Lagrangian,

$$S = \int d^4x\, \underbrace{\mathcal{L}(\{\phi_i\}, \{\nabla_\mu \phi_i\})}_{\text{not scalar}} = \int \underbrace{d^4x\, \sqrt{-|g|}}_{\text{scalar}}\, \underbrace{\hat{\mathcal{L}}(\{\phi_i\}, \{\nabla_\mu \phi_i\})}_{\text{scalar}}, \tag{1.3}$$

⌈Maybe specify that this is only for scalar fields? Or include other fields?⌋

1.1.2 Expanding universe: standard cosmology

- expansion rate, cosmic time, conformal time
- why is flat assumption OK?
- redshift $\mathfrak{z} = a_0/a - 1$

The standard model of cosmology, the ΛCDM

1.1.3 Method of Green's functions

A linear ordinary differential equation (ODE) $\mathrm{L}_x f(x) = g(x)$ assumes a linear differential operator L, a ⌈continuous⌋?, unknown function f, and a right-hand side g that constitutes the inhomogeneous part of the ODE. The *Green's function* G for the ODE (or L) is manifest as any solution to $\mathrm{L}_x G(x, y) = \delta(x - y)$ ⌈check plagiarism (Bringmann)⌋. If L is translation invariant (invariant under $x \mapsto x + a$)—which is equivalent to L having constant coefficients—we can write $G(x, y) = G(x - y)$ and [←show?]■

$$f(x) = (G * g)(x) = \int \mathrm{d}y\, G(x - y)g(y) \tag{1.4}$$

solves $\mathrm{L}_x f(x) = g(x)$.

Let $f_i^{(0)}$, $i = 1, 2, 3, \ldots$ be solutions to the homogeneous ODE, i.e. $\mathrm{L}_x f_i^{(0)} = 0$. Then, by the superposition principle, $f(x) + \sum_i c_i f_i^{(0)}$ is also a solution of the original, inhomogeneous equation.

Pulse signal. Consider the very common scenario where the source is a temporary pulse;

$$g(x) = \begin{cases} g(x), & x_0 \le x \le x_1, \\ 0, & x \ge x_1. \end{cases} \tag{1.5}$$

This is a test.

Part I

Background

Chapter 2

General Relativity

- SECTIONS:

  Differential geometry: The basics, hypersurfaces++, conformal geometry

  Einstein's field equations: How-to, SE tensor

  Gravitational waves: Basics

  Standard model of cosmology: Basics, problems

- AIM: Basis for standard GR

Alongside quantum mechanics, Einstein's theory of gravity—general relativity (GR)—is widely accepted as the most accurate description of our surroundings. GR can be formulated from a geometrical point of view, or it can be viewed as a classical field theory. In the former approach we meet geometrical tools such as the geodesic equation, whereas the latter allows the application of field-theoretical methods.

PHANTOM PARAGRAPH: TWO PERSPECTIVES INSIGHTFUL; BETTER OVERALL UNDERSTANDING OF ASPECTS OF CONCEPTS IN GR

2.1 Differential geometry

To develop a classical field theory, we require a handful of mathematical structures? concepts from differential geometry.

2.1.1 Hypersurfaces

A hypersurface of a $(p+q)$-dimensional manifold $\mathscr{M}$ is a submanifold of codimension 1, i.e. with $p+q-1$ dimensions.

2.1.2 Conformal geometry

- Conformal geometry
- FLRW spacetime & Jordan vs. Einstein frames
- Scale invariance
- Scalar product preserved $\rightsquigarrow$ neat FTs

Fourier transforms

One very neat consequence of this scale invariance is that in FLRW cosmology we can use the regular, flat-space form of the Fourier transform and its inverse:

$$f(x) = \int \frac{d^4k}{(2\pi)^4} \, \mathrm{e}^{-\mathrm{i}\eta_{\mu\nu}k^\mu x^\nu} f(k) \qquad = \int \frac{\mathrm{d}\omega}{2\pi} \, \mathrm{e}^{\mathrm{i}\omega\tau} \int \frac{d^3k}{(2\pi)^3} \, \mathrm{e}^{-\mathrm{i}\boldsymbol{k}\cdot\boldsymbol{x}} f(\omega, \boldsymbol{k}) \tag{2.1a}$$

$$f(k) = \int d^4x \, \mathrm{e}^{\mathrm{i}\eta_{\mu\nu}k^\mu x^\nu} f(x) \qquad = \int \mathrm{d}\tau \, \mathrm{e}^{-\mathrm{i}\omega\tau} \int d^3x \, \mathrm{e}^{\mathrm{i}\boldsymbol{k}\cdot\boldsymbol{x}} f(\tau, \boldsymbol{x}) \tag{2.1b}$$

The four-vectors $[x^\mu] = (\tau, \boldsymbol{x})$ and $[k^\mu] = (\omega, \boldsymbol{k})$ represent the comoving coordinate and wavevector, respectively. **[16, Ch. 17.1]**

⌜Make this readable (typesetting)⌟

2.2 Einstein's equation

How does the gravitational field affect how matter behaves, and in what way is matter controlling the gravitational field? Newtonian gravity proposes very good answers to these questions: The acceleration of an object in a gravitational potential Φ is

$$\boldsymbol{a} = -\boldsymbol{\nabla}\Phi, \tag{2.2}$$

and said field is governed by the matter density ρ through the Poisson equation

$$\boldsymbol{\nabla}^2\Phi = 4\pi G_\mathrm{N}\rho. \tag{2.3}$$

In physics, the answer to a question is highly dependent on *how the question was asked*. A common misconception is that Newtonian gravity was disproven by Einstein. Newton was simply telling a different story; a story about dynamics in non-relativistic systems.[1] Einstein confronted gravitational physics with different but analogous questions, and subsequently more complex answers than Newton. General relativity explains how curvature of spacetime influences matter, manifesting as gravity, and in what way energy and momentum affects spacetime to create curvature. In mathematical terms, these are the geodesic equation

$$\frac{\mathrm{d}^2x^\mu}{\mathrm{d}\lambda^2} = -\Gamma^\mu_{\rho\sigma}\frac{\mathrm{d}x^\rho}{\mathrm{d}\lambda}\frac{\mathrm{d}x^\sigma}{\mathrm{d}\lambda} \tag{2.4}$$

and Einstein's equation

$$\mathcal{G}_{\mu\nu} = 8\pi G_\mathrm{N} T_{\mu\nu}. \tag{2.5}$$

These can be obtained by

⌜Not too long chapter, but want to mention the "naive" tankegang from which these can be obtained (minimal coupling etc.).⌟

[4, Ch. 4]

A more tangible way to obtain the same equation is to vary the combined matter and Einstein–Hilbert actions

$$\boxed{\mathcal{R}_{\mu\nu} - \frac{1}{2}\mathcal{R}g_{\mu\nu} = 8\pi G_\mathrm{N} T_{\mu\nu}.} \tag{2.6}$$

[1] Which, to be fair, are most common on Earth.

DRAFT

The Einstein–Hilbert action in vacuum is ⌜check Planck mass def.⌟

$$S_{\mathrm{EH}} = {}^{1}\!/_{2} M_{\mathrm{Pl}}^2 \int d^4x \, \sqrt{-|g|}\,\mathcal{R}, \tag{2.7}$$

where $\mathcal{R} = g^{\mu\nu}\mathcal{R}_{\mu\nu}$. By varying S_{EH} with respect to $g_{\mu\nu}$ one obtains the equation of motion

$$\mathcal{G}_{\mu\nu} \equiv \mathcal{R}_{\mu\nu} + \frac{1}{2} g_{\mu\nu}\mathcal{R} = 0. \tag{2.8}$$

Thus, we interpret GR as a *classical* field theory where the tensor field $g_{\mu\nu}$ is the gravitational field, ⌈with the particle realisation named "graviton"⌋◡.

Einstein's equation for general relativity

$$\boxed{\mathcal{R}_{\mu\nu} - \frac{1}{2}\mathcal{R} g_{\mu\nu} = 8\pi G_{\mathrm{N}} T_{\mu\nu}.} \tag{2.9}$$

2.3 Standard model of cosmology

Employing the cosmological principle (CP) to the Einstein equation, simplifies them drastically. CP states that universe is spatially homogeneous and isotropic⌈—some "folkelig" comment—⌟or equivalently that the line element of the universe takes the form $ds^2 = -\mathrm{d}t^2 + a^2(t)d\Sigma^2$ where $d\Sigma$ is a three-dimensional metric with a specified Gaussian curvature. a is the scale factor describing the universe's expansion. This was the starting point for Alexander Friedmann when he ⌈utformet⌋◡ the Friedmann equations. If CP holds, any constituent s behaves as a perfect fluid, and the Hubble parameter reads ⌈decide which here⌟

$$H^2 = H_0^2 \sum_s \Omega_{s0} a^{-3(1+w_s)}, \tag{2.10}$$

$$\mathcal{H}^2 = H_0^2 \sum_s \Omega_{s0} a^{-(1+3w_s)}, \tag{2.11}$$

where w_s is the equation-of-state parameter of s.

CP + EFEs = FI & FII

CP holds for scales $> \mathcal{O}(100$ Mpc$)$

⌈Get to Hubble tension.⌟

We will work with conformal time τ that relates to cosmic time t such that the metric is

$$ds^2 = a^2(-\mathrm{d}\tau^2 + \mathrm{d}\Sigma^2). \tag{2.12}$$

To get simplified—or simply analytically solvable—equations, we often assume $a \sim \tau^\alpha$ that corresponds to a universe dominated by a single substance. α is eventually determined by the equation-of-state parameter w_s associated with the substance s in question,

$$\alpha = \frac{2}{1 + 3w_s}. \tag{2.13}$$

This means that $\alpha = 1$ and $\alpha = 2$ for radiation (RD) and matter domination (MD), respectively. Put in cosmic context, ⌜maybe have a figure? Or write something about the different eras?⌟

2.3.1 Cosmological perturbation theory

Just look around you—the universe is definitely *not* homogeneous and isotropic. The story of structure formation as we know it is told through cosmological perturbation theory. The leading-order perturbed metric $\mathring{g}_{\mu\nu} = g_{\mu\nu} + \delta g_{\mu\nu}$ can be written in terms of functions A, B_i and C_{ij},

$$d\mathring{s}^2 = a^2\Big[-(1 + 2A)\mathrm{d}\tau^2 + 2B_i\mathrm{d}x^i\mathrm{d}\tau + (\delta_{ij} + C_{ij})\mathrm{d}x^i\mathrm{d}x^j\Big]. \tag{2.14}$$

It is convenient to adopt the convension that spatial vectors and tensors are raised and lowered with δ, e.g. $C^{ij} = \delta^i_k\delta^j_l C_{kl}$. The symmetric metric has ten degrees of freedom, and a scalar-vector-tensor (SVT) decomposition separates these into four scalar, four vector and two tensor degrees of freedom:

$$A \to A, \tag{2.15a}$$
$$B_i \to \partial_i B + F_i, \tag{2.15b}$$
$$C_{ij} \to (2\delta_{ij}C + 2\partial_i\partial_j D - (2/3)\delta_{ij}\boldsymbol{\nabla}^2 D) + 2\partial_{(i}G_{j)} + 2E_{ij}. \tag{2.15c}$$

This is extremely useful since in the first-order linearised Einstein equation for scalars, vectors and tensors do not mix. We treat these separately and assume they originate from inflation.

- Scalar perturbations (A, B, C, D) are density perturbations and describe structure formation.
- Vector perturbations (F_i, G_i) are not predicted by inflation, and would in any case only have decaying solutions, and are thus cosmologically irrelevant.
- Tensor perturbations (E_{ij})—gravitational waves—are predicted by inflation.

This thesis focuses solely on the tensorial part of the metric perturbation. Therefore, we will consider the divergence- and traceless $h_{ij} = 2E_{ij}$. This particular choice is called the *transverse-traceless* (TT) gauge; $\partial^i h_{ij} = 0$ and $\delta^{ij}h_{ij} = 0$. Any symmetric tensor T_{ij} can be projected onto the TT-gauge by use of the projection tensor in Eq. (2),

$$T^{\mathrm{TT}}_{ij}(\boldsymbol{k}) = \Lambda^{ij}{}_{kl}(\boldsymbol{k}/k)T_{kl}(\boldsymbol{k}). \tag{2.16}$$

2.3.2 Hubble trouble

- Hubble tension
- Flatness problem
- Extended models of gravity
- ΛCDM still very good!

In combining the distance to a nearby galaxy and the rate at which it moves away from us, we find the expansion rate of the universe

In short, local measurements suggests $h_0 \simeq 0.73$, but CMB observations will have it $h_0 \simeq 0.67$. The measurement errors cannot explain this.

2.4 Linearised gravity; tensor sector

Applying perturbation theory to the metric gives rise to a new set of equations, often referred to as the "linearised Einstein field equations." The general starting point is to expand the metric to the order o in question $\mathring{o}$,

$$\mathring{g}_{\mu\nu} = g_{\mu\nu} + \sum_{i=1}^{o} \delta^{(i)} g_{\mu\nu}. \tag{2.17}$$

Consequently, the perturbed Einstein reads

$$\mathring{\mathcal{G}}_{\mu\nu} = 8\pi G_{\text{N}} \mathring{T}_{\mu\nu}, \tag{2.18}$$

where $\mathring{\mathcal{G}}_{\mu\nu} = \sum_{i=0}^{o} {}^{(0)}\mathcal{G}_{\mu\nu}$ and $\mathring{T}_{\mu\nu} = \sum_{i=0}^{o} {}^{(0)}T_{\mu\nu}$, in which ${}^{(i)}Q$ implies the perturbed quantity to order o. It is then solved order by order. ⌜Either put details in appendix or refer to e.g. Jokela et al. [13]⌟

PHANTOM PARAGRAPH: About gauge freedom, TT gauge etc.—why "waves"

Metric perturbations on a homogeneous and isotropic background leaves two tensor degrees of freedom. We extract these by use of the spin-2 projection tensor On the Transverse-Traceless Projection in Lattice Simulations of Gravitational Wave Production

2.4.1 Gravitational waves in an expanding universe

We are interested in a flat FRLW background plus first order in perturbations, and define the perturbed metric as $\mathring{g}_{\mu\nu} = a^2(\eta_{\mu\nu} + h_{\mu\nu})$. Furthermore, we focus on the tensorial part of the perturbations

$$\mathring{ds}^2 = a^2(\tau)\Big(-\mathrm{d}\tau^2 + \big[\delta_{ij} + h_{ij}(\tau, \boldsymbol{x})\big]\mathrm{d}x^i \mathrm{d}x^j\Big) \tag{2.19}$$

blah blah [...]

$$\Box h_{ij}(\tau, \boldsymbol{x}) = -16\pi G_{\text{N}} a^2 T_{kl}(\tau, \boldsymbol{x}) \tag{2.20}$$

For notational ease, we define $S_{ij} \equiv 16\pi G_{\text{N}} T_{ij}$ and omit the lower indices. In real space, the equation reads

$$\ddot{h} + 2\mathcal{H}\dot{h} - \boldsymbol{\nabla}^2 h = S, \tag{2.21}$$

which in its homogeneous form is we recognise as a damped harmonic oscillator. It is convenient to transform to Fourier space where $k_i \leftrightarrow \mathrm{i}\partial_i$, and even more so to introduce $\bar{h} \equiv ah$, leaving us with

$$\ddot{\bar{h}} + \left(k^2 - \frac{\ddot{a}}{a}\right)\bar{h} = aS. \tag{2.22}$$

We see that for large modes $k \gg \ddot{a}/a \sim \tau^{-2}$, the linear operator is approximately $\partial_\tau^2 + k^2$, i.e. the harmonic oscillator, with plane wave solutions for $S = 0$. That is to say, small-scale gravitational waves, in the absence of a source, propagate free waves in an FRW spacetime (divided by the scale factor). On larger scales, the propagation is damped in accordance with the expansion of the universe. This damping term generally depends on expansion history.

Homogeneous solution. We see that for large modes $k^2 \gg \ddot{a}/a \sim \tau^{-2}$, the general solution

Inhomogeneous solution. The method of Green's functions presents a suitable recipe for determining the dynamics of tensor perturbations on an expanding background. There are some limitations, however, as to the analytical solvability of the system. In the small-scale limit, the damping is neglected, and we only need the retarded Green's function associated with the harmonic oscillator, $\sin(k(\tau - \tau'))/k$. Otherwise, an equation of the form $\mathrm{L}_{u=k\tau} h = aS/k^2$, where

$$\mathrm{L}_u = \frac{\mathrm{d}^2}{\mathrm{d}u^2} + \left(1 - \frac{(\alpha-1)\alpha}{u^2}\right) \tag{2.23}$$

has a Green's function in terms of Bessel functions $\sqrt{u}\mathsf{Z}_{\alpha-1/2}(u)$, which is the case in a single-substance universe with $a \propto \tau^\alpha$. On an even more compact form, if $n \equiv \alpha - 1 \in \mathbb{Z}$, we can use the Green's function

$$G(u, v) = \mathsf{S}_n(u)\mathsf{C}_n(v) - \mathsf{C}_n(u)\mathsf{S}_n(v)\chi\Lambda \tag{2.24}$$

where $\mathsf{S}_n(x)$ and $\mathsf{C}_n(x)$ are the Riccati–Bessel and –Neumann functions (given in Appendix C).

Assume homogeneous initial conditions, $\bar{h}(\tau_{\text{init}}, \boldsymbol{k}) = \dot{\bar{h}}(\tau_{\text{init}}, \boldsymbol{k}) = 0$. The full solution is as follows:

$$h_{ij}(\tau, \boldsymbol{k}) = \frac{16\pi G_{\text{N}}}{k^2} \int_{\tau_{\text{init}}}^{\tau} \mathrm{d}\eta\, G(k\tau, k\eta) \frac{a(\eta)}{a(\tau)} T_{ij}(\eta, \boldsymbol{k}). \tag{2.25}$$

2.4.2 Polarisation of tensor modes / TITLE (Effect on test particles)

PHANTOM PARAGRAPH: A LONGER DISCUSSION—SPECIFIC TO GR

From the right-handed orthonormal basis $\{\hat{\boldsymbol{m}}, \hat{\boldsymbol{n}}, \hat{\boldsymbol{\Omega}}\}$—for which $\hat{\boldsymbol{\Omega}} \parallel \boldsymbol{k}$—we may construct a linear polarisation basis from the polarisation tensors

$$\begin{aligned} e^{+}(\hat{\boldsymbol{\Omega}}) &= \hat{\boldsymbol{m}} \otimes \hat{\boldsymbol{m}} - \hat{\boldsymbol{n}} \otimes \hat{\boldsymbol{n}} \quad \text{and} \\ e^{\times}(\hat{\boldsymbol{\Omega}}) &= \hat{\boldsymbol{m}} \otimes \hat{\boldsymbol{n}} - \hat{\boldsymbol{n}} \otimes \hat{\boldsymbol{m}}. \end{aligned} \tag{2.26}$$

This is a popular choice, and it blah blah [...]

Now we retrieve

$$h_{ij}(\tau, \boldsymbol{k}) = \sum_{P=+,\times} h_P(\tau, k\hat{\boldsymbol{\Omega}}) e^P_{ij}(\hat{\boldsymbol{\Omega}}) \tag{2.27}$$

and observe that

$$\left|h^2(\tau, \boldsymbol{k})\right| = \sum_{ij} h^{ij}(\tau, \boldsymbol{k}) h_{ij}(\tau, \boldsymbol{k}) = 2 \sum_P h_P^2(\tau, \boldsymbol{k}). \tag{2.28}$$

monochromatic+: O-I-O-Å, ... monochromatic ×: Michael Jackson dance?

Chapter 3

TITLE (Kinks in Cosmology)

PHANTOM PARAGRAPH: ABOUT MODIFIED GRAVITY ETC.

Candidate theories for physics beyond the ΛCDM model include modified gravity theories and quintessence. A possible consequence of theories that predicts phase transitions is the creation of topological defects such as cosmic strings and domain walls.

PHANTOM PARAGRAPH: REASON FOR MODIFICATION—AUXILIARY SCALAR FIELDS AND EXPANSION

- SECTIONS:

  Quintessence: Auxiliary fields

  Domain walls:

3.1 TITLE (Topological defects)

- Cover: motivation, classical kink solution (+ translational symmetry +antikinks+ series of kinks)
- about topological solitons / defects
- symmetry breaking
- Properties: NG action, width, mass/tension

PHANTOM PARAGRAPH: ABOUT TOPOLOGICAL DEFECTS

⌈Kink solutions placed in spacetime with more than one spatial dimension, they become extended, planar structures (or membranes), that which we call "domain walls". [19]⌋ Domain walls possess richer dynamics than kinks, and blah blah [. . .]

Is there a difference between topological solitons and topological defects?

The only type of topological defect that is directly relevant to this project is the domain wall, specifically the Z_2 type. These are two-dimensional topological defects that occurs where a discrete symmetry is broken.[1]

To give an idea of the basic properties of topological defects, we present an example. More thorough derivations can be found in Vachaspati [19]. ⌈Later on, we will derive it for DWs in FRW spacetime.⌋

[1] Likewise, cosmic strings and monopoles are products of axial/cylindrical and spherical symmetry breaking, respectively.

3.1.1 Example: (stationary) $\mathbb{Z}_2$ kinks

The king of kinks, the so-called "$\mathbb{Z}_2$ kink," can be described through a scalar field ϕ with the action $S = S_{\text{EH}} + S_{\mathbb{Z}_2}$,

$$S_{\mathbb{Z}_2} = \int d^{n+1}x \sqrt{-g}\left\{-\frac{1}{2}g^{\mu\nu}\partial_\mu\phi\partial_\nu\phi - V(\phi)\right\}, \tag{3.1}$$

where $V(\phi)$ is the two-fold degenerate potential $V(\phi) = \lambda(\phi^2 - \eta^2)^2$. The eom $\Box\phi = V_{,\phi}$ can be derived from variation of S with respect to ϕ. For simplicity, we consider Minkowski spacetime with $1 + 1$ dimensions where $\eta_{\mu\nu} = \text{diag} = (-1, 1)$ is the metric. The eom reads

$$-\partial_t^2\phi + \partial_x^2\phi = \lambda(\phi^2 - \eta^2)\phi. \tag{3.2}$$

Setting time derivatives to zero, and imposing boundary conditions $\phi(x \to \pm\infty) = \pm\eta$, we obtain a class of static solutions

$$\phi_{\text{k}}(x; x_0) = \eta \tanh\left(\sqrt{\frac{\lambda}{2}}\eta(x - x_0)\right), \tag{3.3}$$

where x_0 is the position of the kink. ⌜Translational invariance $\phi_{\text{k}}(x; x_0) = \phi_{\text{k}}(x - x_0)$⌟

Multi-kink field. Without commenting further, we state that this kink has *topological charge* $Q = 1$ (Vachaspati [see 19, Ch. 1] for discussion). This comes from the boundary conditions, and thus similar arguments constructs solutions with $Q = -1$ by swapping the boundaries; $\phi(x \to \pm\infty) = \mp\eta$. This is the *antikink* solution $\overline{\phi}_{\text{k}}(x) = -\phi_{\text{k}}(x)$. A feature of the $\mathbb{Z}_2$ kinks is that one cannot have a system with topological charge $|Q| > 1$. For sufficiently separated kinks and antikinks located at x_i and $\overline{x}_j$, respectively, we write [19]:

$$\phi(x) = \frac{\eta}{\eta^{N+M}}\prod_i^N \phi_{\text{k}}(x - x_i)\prod_j^M \overline{\phi}_{\text{k}}(x - \overline{x}_j), \tag{3.4}$$

where $|N - M| \leq 1$ and $x_i < \overline{x}_j < x_{i+1}$. This describes the allowed system of N kinks and M antikinks aligned in an alternating structure.

Basic properties

The energy of the kink is obtained integrating over the energy density, i.e.

$$E = \int \mathrm{d}x\, T^0{}_0 = \frac{2\sqrt{2}}{3}\lambda\eta^3. \tag{3.5}$$

⌜Check sign.⌟ We define the width of the kink to be the argument where the tanh function equals $\tanh 1/\sqrt{2}$,

$$w = \frac{1}{\eta\sqrt{\lambda}}. \tag{3.6}$$

Most of the energy is confined within $x \in x_0 + [-w/2, w/2]$. See Section 3.1.1 for illustrative explanation.

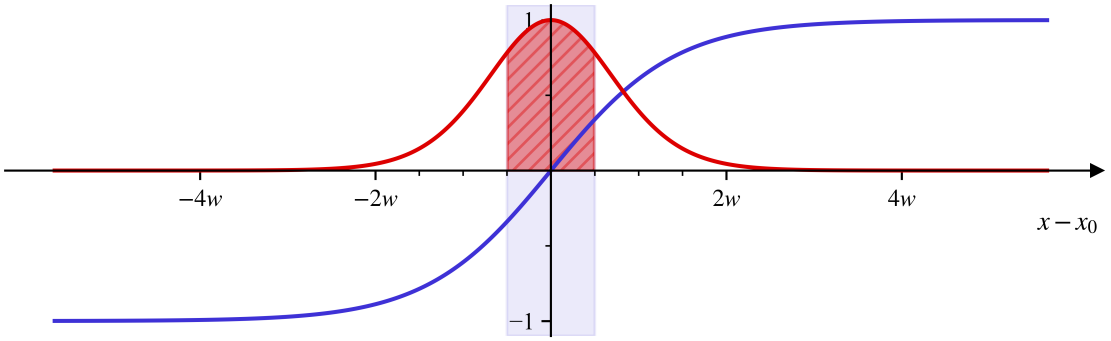

Figure 3.1: Demonstration of the $\mathbb{Z}_2$ kink blah blah [...].

3.1.2 TITLE (Domain walls)

The kink solution in Section 3.1.1 put in two more spatial dimensions (setting $\eta_{\mu\nu} = \text{diag}(-1, 1, 1, 1)$) is a planar $\mathbb{Z}_2$ domain wall. The energy in Eq. (3.5) is now a surface energy density better known as the *surface tension* of the wall, denoted σ.

For later convenience, we will define σ_∞ and δ_∞ as the surface tension and wall width as their solutions in the stationary $\mathbb{Z}_2$ scenario, respectively. In terms of the mass scale $\mu = \eta\sqrt{\lambda}$, this amounts to

$$\sigma_\infty \equiv \frac{2\sqrt{2}}{3}\frac{\mu^3}{\lambda} \quad \text{and} \quad \delta_\infty \equiv \frac{1}{\mu}.^2 \tag{3.7}$$

PHANTOM PARAGRAPH: NAMBU-GOTO ACTION

3.1.3 Defect formation

⌜Maybe own section?⌟

- Effective potential
- First-order phase transitions
- Biased phase transitions?

Defect formation, symmetry breaking and phase transitions are tightly related phenomena. ⌜Write in general terms.⌟ To study phase transitions it is helpful to use the *effective potential* that takes into account the interaction between some field and a background. An effective potential can ensure that a scalar field does not really show itself until some critical point at which the vacuum state goes from being trivial to blah blah [...]

Energy bias

Existence of discrete vacua implicates existence of domain walls. The degeneracy of these vacua ensures the stability of such walls. If we imagine a slight break in this degeneracy, that is, if one vacuum is favoured over another, biased domain walls form [19]. blah blah [...]

[2] In Part II, we set $\phi_\infty = \eta$.

3.2 TITLE (Quintessence)

The general picture presents quintessence as a group of scalar–tensor theories; a subgroup of modifications to gravity in which a scalar field is added to the total action. By going through all possible covariants with maximum second order time derivatives in four dimensional spacetime, one arrives at the most general formulation of these type of theories, the *Hordenski theory*. Said theory is summed up by the total Lagrangian density $\mathcal{L}_{\mathrm{H}} = \mathcal{L}_{\mathrm{m}} + M_{\mathrm{Pl}}^2 \sum_{i=2}^{5} \mathcal{L}_i$, where $\mathcal{L}_i$ are built up by derivatives of the scalar field, the Einstein tensor and arbitrary functionals of the scalar field ϕ and its kinetic term $X = -{}^1\!/_2 \phi^{;\mu}\phi_{;\mu}$.[3] Let $\mathcal{L}_i = 0$ as a starting point. General relativity—represented by the Einstein–Hilbert action—is retrieved with $\mathcal{L}_4 = \mathcal{R}/2$. By also setting $\mathcal{L}_2 = X(\phi) - V(\phi)$, we get a quintessence model. Performing relevant variations eventually gives an equation of motion that is indistinguishable from standard GR with $\mathcal{L}_{\mathrm{m}} \to \mathcal{L}_{\mathrm{m}} + \mathcal{L}_2$ in the stress–energy tensor on the rhs of the Einstein equation. Thus, quintessence models are not actually modified gravity theories, but adds to the total matter in the universe. [5]

3.2.1 General framework

We go through the dynamics of a quintessence field ϕ that is associated with a kinetic term $X = -{}^1\!/_2 g^{\mu\nu}\phi_{;\mu}\phi_{,\nu}$ and potential energy $V(\phi)$ in rough stages. This will lay the foundation for ⌜symmetron etc.⌟

Conformal duality. We argued in Section 2.1.2 that ⌜observables are preserved under conformal transformations of the metric.⌟? ⌜Short text about Jordan and Einstein frames.⌟

The dynamics of the quintessence field ϕ is described by the action

$$S = \int d^4x \sqrt{-g} \left\{ \frac{M_{\mathrm{Pl}}^2}{2}\mathcal{R} + X(\phi) - V(\phi) \right\} + S_{\mathrm{m}}[\tilde{g}_{\mu\nu}, \psi] \tag{3.8}$$

in the Einstein frame. Without the presence of the last term, the eom for the scalar field is $\Box\phi = V_{,\phi}$. Some article© (appendix?) shows that the minimal coupling to matter contributes s.t. $\Box\phi \supset -A^{-1}A_{,\phi}T_{\mathrm{m}}$, which amounts to writing

$$\Box\phi = V_{\mathrm{eff},\phi}; \quad V_{\mathrm{eff}}(\phi) = V(\phi) - \ln A(\phi) \cdot T_{\mathrm{m}}. \tag{3.9}$$

For a perfect fluid, $T_{\mathrm{m}} = -\rho + 3p$.

Fifth force. Matter particles in the Jordan frame obey the simple geodesic equation as there is no coupling to ϕ. On the other hand, particles in the Einstein frame matter sector experience a *fifth force* due to the universal coupling. The fifth force concept captures the non-trivial rhs of in the geodesic equation,⌜

$$\ddot{\boldsymbol{x}} \supset \frac{\boldsymbol{F}_5}{m} = -\frac{\beta}{M_{\mathrm{Pl}}}\boldsymbol{\nabla}\phi. \tag{3.10}$$

⌟? β is then a measure of the strength of the fifth force relative to the Newtonian gravitational force. ⌜Violation of WEP. Maybe refer to equations in Section 2.2?⌟

[3] With the usual notation convention and arbitrary functionals G_i, the Lagrangian densities $\mathcal{L}_i$ are given by the following:

$$\begin{aligned}
\mathcal{L}_2 &= G_2(\phi, X), \\
\mathcal{L}_3 &= G_3(\phi, X)\Box\phi, \\
\mathcal{L}_4 &= G_4(\phi, X)\mathcal{R} + G_{4,X}(\phi, X)\Big((\Box\phi)^2 - \phi_{;\mu\nu}\phi^{;\mu\nu}\Big), \\
\mathcal{L}_5 &= G_5\mathcal{G}_{\mu\nu}\phi^{;\mu\nu} - {}^1\!/_6 G_{5,X}(\phi, X)\Big((\Box\phi)^3 + 2\phi^{\nu}{}_{;\mu}\phi^{\mu}{}_{;\nu} - 3\phi_{;\mu\nu}\phi^{;\mu\nu}\Box\phi\Big),
\end{aligned}$$

where $G_{i,X} = \partial G_i/\partial X$.

Screening.

3.2.2 Asymmetron model

The particular quintessence model characterised by the symmetric Mexican-hat potential

$$V(\phi) = \frac{\lambda}{4}\phi^4 - \frac{\mu^2}{2}\phi^2 + V_0 \tag{3.11}$$

is called the *symmetron model*. This theory is invariant under change of sign ⌜reflection⌟, $\phi \to -\phi$, (ϕ is Z_2 symmetric) a requirement from quantum theory.[©] Not equally well-established is the generalisation of this model called the *a*symmetron, in which the potential is given an additional cubic term, $V(\phi) \supset -\kappa\phi^3/3$. Here, one of the domains is favoured over the other.

Now, why would we want this asymmetry in the first place? It complicates things by breaking the Z_2-symmetry of the symmetron, so the theory only holds approximately. However, this asymmetry can aid in overcoming the domain wall problem. ⌜Overclosing the universe.⌟

Note that introducing asymmetry in this way is different from energy bias in the sense that not only is the energy in the two domains different, but the expectation values for ϕ are shifted.

The simplest symmetron model has the quadratic coupling

$$A(\phi) = 1 + \frac{1}{2}\left(\frac{\phi}{M}\right)^2 + \mathcal{O}\left((\phi/M)^4\right). \tag{3.12}$$

The effective potential is then given by [11]

$$\boxed{V_{\text{eff}}(\phi) = \frac{\lambda}{4}\phi^4 - \frac{\kappa}{3}\phi^3 + \frac{\mu^2}{2}\left(\frac{\rho}{\mu^2 M^2} - 1\right)\phi^2 + V_0.} \tag{3.13}$$

This potential becomes unstable when $\rho \le \mu^2 M^2 \equiv \rho_*$, and the field rolls into either of the two vacua. From the cosmological perspective, ignoring κ, we imagine an initially dense region in the universe where a scalar field oscillates slightly around zero. The energy density dilutes and eventually reaches $\rho = \rho_*$, spontaneously breaking the Z_2-symmetry, and separates the scalar field into domains according to their sign at the time. The potential barriers created at this *phase transition* correspond to the topological solitons discussed in Section 3.1; namely cosmic domain walls.

Let $\upsilon \equiv \rho_{\text{m}}/(\mu^2 M^2)$. By setting $V_{\text{eff},\phi} = 0$, we find the vacuum expectation values

$$\phi_0 = 0 \quad \vee \quad \phi_\pm = \phi_\infty\left(\bar{\kappa} \pm \sqrt{\bar{\kappa}^2 + 1 - \upsilon}\right), \tag{3.14}$$

where we defined $\bar{\kappa} = \kappa/(2\mu\sqrt{\lambda})$ and $\phi_\infty = \mu/\sqrt{\lambda}$. Note that for the symmetron ($\kappa = 0$), since the field is real, VEV is zero before SSB. We determine the stability of these vacua by evaluating $V_{\text{eff},\phi\phi}$ at $\phi = \phi_0, \phi_\pm$ and see that ϕ_0 remains stable until ρ_*.

Parameters

PHANTOM PARAGRAPH: PARAMETER SPACE OF ASYMMETRON

- Phase transition aspect
- Screening
- Comment on asymmetron

Burrage et al. [3] sets the constraint $M \lesssim 10^{-3.6} M_{\text{Pl}}$

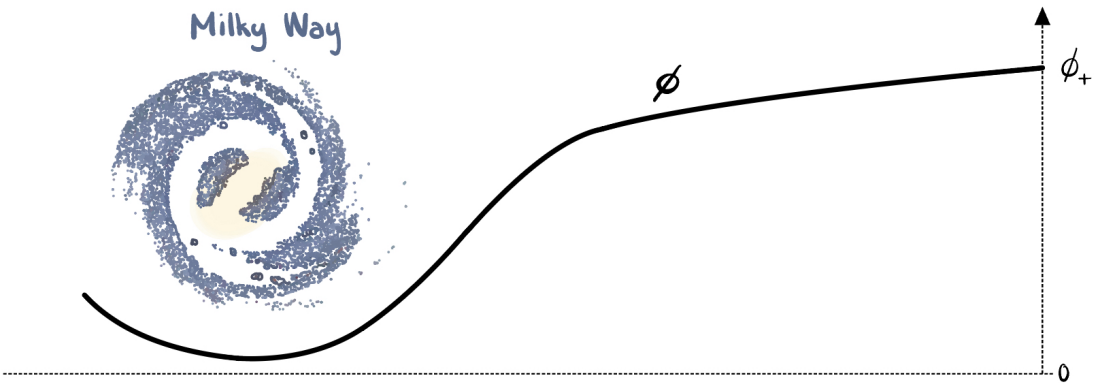

Figure 3.2: Schematic of the symmetron screening mechanism. It is clear that the vacuum expectation value goes to zero in dense regions.

Part II

Methodology

Chapter 4

Imperfect Defects

Any cosmologically relevant domain wall will be thin compared to the horizon. Are they sufficiently thin so that the thin-wall approximation holds? If so, we should be able to study the dynamics of such walls by viewing them as $(2 + 1)$-dimensional timelike hypersurfaces in a spacetime of $3 + 1$ dimensions. We can find an eom for leading order distortions to the wall normal coordinate, eventually feeding asymmetry to the Nambu–Goto stress–energy tensor (Section 3.1), necessarily causing spacetime distortions that may or may not live on to paint its autograph in a gravitational wave observation on Earth. How this signature looks, is for us to figure out.

PHANTOM PARAGRAPH: MOTIVATION–INSPIRATION(WORK)

We will in this chapter explore the dynamics of domain walls in the thin-wall limit, where the emphasis is not on the scalar field χ, but of the position and evolution of the domain wall itself.

To substantiate the applicability of this theory, we begin in a more general picture than what we eventually will need. We consider a d-dimensional timelike submanifold Σ embedded in smooth Riemannian manifold $\mathscr{M}$ of one time dimension and $n - 1$ spatial dimensions. We let Σ have codimension one and split the ambient space into two separate hypervolumes. Now, Σ is a timelike hypersurface of $\mathscr{M}$ that can be interpreted as the n-dimensional analog of an infinitely thin domain wall.

4.1 TITLE (Kink dynamics / General formula)

- Vary DW action
- Goal: E.O.M. for physically relevant component (epsilon basically)
- Expression for energy–momentum tensor
- Extension to non-thin walls
- Extension to Asymmetron or introduction of energy bias
- What does thin mean? Why is the tension indep. of width?

In this fairly technical section we follow Garriga and Vilenkin [10] and Ishibashi and Ishihara [12]. In mathematical terms, we consider a smooth spacetime

$$\mathscr{M} = (\mathbb{R}^{n-1,1}, g_{\mu\nu}) \supset \Sigma = (\mathbb{R}^{d-1,1}, \gamma_{ab}) \tag{4.1}$$

where $d = n - 1$ and indices $a, b, c = 0, 1, \ldots d - 1$, while Greek indices as usual runs from 0 to $n-1$. Let the world sheet Σ divide $\mathscr{M}$ into two hypervolumes $\mathscr{M}_\pm$ such that $\mathscr{M} = \mathscr{M}_+ \cup \Sigma \cup \mathscr{M}_-$. We invoke a smooth coordinate system $\{x^\mu\}$ of the spacetime in a neighbourhood of Σ. The embedding of Σ in $\mathscr{M}$ is $x^\mu = x^\mu(\xi^a)$, where the coordinate system $\{\xi^a\}$ parametrises Σ. The induced metric on Σ is

$$\gamma_{ab} = g_{\mu\nu} e^\mu_a e^\nu_b; \quad e^\mu_a \equiv x^\mu{}_{,a} = \frac{\partial x^\mu}{\partial \xi^a}. \tag{4.2}$$

[←argue!]■ e^μ_a are the tangent vectors and n^μ the unit normal vector pointing from Σ to $\mathscr{M}_+$, obeying

$$g_{\mu\nu} n^\mu n^\nu = 1 \quad \text{and} \quad g_{\mu\nu} e^\mu_a n^\nu = 0. \tag{4.3}$$

The action for the system is [12]

$$S = -\sigma \int_\Sigma d^d\xi \sqrt{-\gamma} - v_+ \int_{\mathscr{M}_+} d^n x \sqrt{-g} - v_- \int_{\mathscr{M}_-} d^n x \sqrt{-g}\,. \tag{4.4}$$

The first term is the Nambu–Goto action S_{NG} from before$^{\copyright}_{()}$, with σ representing the constant positive energy density of the defect in its rest frame. The rest is the vacuum action S_{vac} given through the constant potential energy densities $v_\pm$ of $\mathscr{M}_\pm$.

Let us consider the variation of S under small changes in the world sheet, $x^\mu \to x^\mu + \delta x^\mu$. Since only transverse motion is physically relevant, we can write the variation in terms of the small, but otherwise arbitrary, function $\psi(\xi^a)$;

$$x^\mu \to x^\mu + \psi n^\mu. \tag{4.5}$$

The eom for the wall normal coordinate is then [10, 12]

$$n_\mu \widehat{\Box} x^\mu + n_\mu \Gamma^\mu_{\kappa\tau} \gamma^{ab} e^\kappa_a e^\tau_b + \frac{v}{\sigma} = 0, \tag{4.6}$$

where $v = v_+ - v_-$, $\widehat{\Box}$ is the d'Alembertian associated with Σ,[1] and $\Gamma^\mu_{\kappa\tau}$ are the spacetime Christophel symbols. This can be written in the simple form

$$\gamma^{ab} \widehat{K}_{ab} = -\frac{v}{\sigma}, \tag{4.7}$$

where the extrinsic curvature tensor is

$$\widehat{K}_{ab} = -e^\mu_a e^\nu_b \nabla_\nu n_\mu. \tag{4.8}$$

In Garriga and Vilenkin [10] it is shown that a planar domain wall oriented perpendicular to the z axis in Minkowski space follows the trajectory $z = z(t)$ whose eom is

$$\frac{z_{,tt}}{(1 - z^2_{,t})^{3/2}} = \frac{v}{\sigma}. \tag{4.9}$$

With $v = 0$ the solution is $z(t) = 0$ in a suitable Lorentz frame. ⌜Comment about constant velocity?⌟

4.1.1 Linearised perturbations

PHANTOM PARAGRAPH: TO LINEAR PERT.

[1] $\widehat{\Box} = \widehat{\nabla}^a \widehat{\nabla}_a = \frac{1}{\sqrt{-\gamma}} \partial_a (\sqrt{-\gamma} \gamma^{ab} \partial_b)$, $\gamma = \widehat{g}$.

4.1.2 Energy and momentum

From the Nambu–Goto action S_{NG}, we can construct an energy–momentum tensor

$$T^{\mu\nu}\big|_{\text{NG}} = \frac{2}{\sqrt{-g}}\frac{\delta S_{\text{NG}}}{\delta g_{\mu\nu}}. \tag{4.10}$$

By rewriting the action to the spacetime integral

$$S_{\text{NG}} = -\sigma \int d^n x \sqrt{-\gamma}\,\delta(r); \quad r \equiv n_\mu x^\mu - x_\perp, \tag{4.11}$$

where the Dirac delta function essentially eliminates any spacetime event that is *not* the defect. The variation $g_{\mu\nu} \to g_{\mu\nu} + \delta g_{\mu\nu}$ gives [19]

$$T^{\mu\nu}\big|_{\text{NG}} = \frac{\sigma}{\sqrt{-g}} \int d^d\xi\ \sqrt{-\gamma}\gamma^{ab} X^\mu{}_{,a} X^\nu{}_{,b}\,\delta(r), \tag{4.12}$$

or

$$T^{\mu\nu}\big|_{\text{NG}} = \frac{\sigma\delta(r)}{\sqrt{-g}\sqrt{-\gamma}}\frac{\delta\gamma}{\delta g_{\mu\nu}}. \tag{4.13}$$

Maybe define $T^{\mu\nu}_{\text{w}}$ or $W^{\mu\nu}$?

TITLE (**Thickness?**)

To some extent, we can account for a possibly non-vanishing wall half-width l by choosing a Gaussian function instead of a Dirac delta distribution. Simply substituting

$$\delta(r) \to \Phi_l(r) = \frac{1}{\sqrt{2\pi}l}\exp\left\{-\frac{r^2}{2l^2}\right\} \tag{4.14}$$

in Eq. (4.13) does the trick, and restores δ in the limit where $l \to \infty$. Note that this is not the same as going beyond the thin-wall limit, but rather an approximation that includes a thickness that is small enough to not alter the dynamics.

4.2 Dynamics of planar domain walls in expanding universe

Now the groundwork is laid for the scenario that which this project is all about. That is, we consider a conformally flat spacetime with line element

$$ds^2 = g_{\mu\nu}\mathrm{d}x^\mu \mathrm{d}x^\nu = a^2\eta_{\mu\nu}\mathrm{d}x^\mu \mathrm{d}x^\nu = a^2(\tau)\left\{-\mathrm{d}\tau^2 + \mathrm{d}x^2 + \mathrm{d}y^2 + \mathrm{d}z^2\right\}. \tag{4.15}$$

We place a thin domain wall at z-coordinate z_0, represented by a hypersurface Σ, whose induced metric is $\gamma_{ab} = g_{\mu\nu}x^\mu{}_{,a}x^\nu{}_{,b}$. We assert the solution $x^\mu \supset x_\perp(\tau)n^\mu = z_0\delta^{\mu z}$ to Eq. (4.7) with $v = 0$.[2]

The perturbed equation is obtained by a similar action principle as before,

$$x^\mu \to \mathring{x}^\mu = x^\mu + \epsilon n^\mu. \tag{4.16}$$

We simplify our equations tremendously if we keep n^μ unaffected by the variation, and solve the one-dimensional problem with

$$x_\perp \to \mathring{x}_\perp = x_\perp + \epsilon. \tag{4.17}$$

[2] In Garriga and Vilenkin [10] it is shown that $z = z_0$ is the only viable solution in the analogous case in Minkowski space.

The resulting equation of motion for the scalar perturbation reads

$$a^2\widehat{\Box}\epsilon - 2\mathcal{H}\dot{\epsilon} = 0 \tag{4.18}$$

or

$$\epsilon_{,\tau\tau} + 3\mathcal{H}\epsilon_{,\tau} - \epsilon_{,xx} - \epsilon_{,yy} = 0. \tag{4.19}$$

This is a separable partial differential equation (PDE) and we assume solutions of the form $\epsilon(\tau, x, y) = \varepsilon(\tau)\mathscr{E}(x, y)$. Now, we separate Eq. (4.19) into

$$\ddot{\varepsilon} + f(\tau)\dot{\varepsilon} + p^2\varepsilon = 0 \quad \text{and} \quad \mathscr{E}_{,xx} + \mathscr{E}_{,yy} + p^2\mathscr{E} = 0, \tag{4.20}$$

where $f(\tau) = 3\mathcal{H}$. The spatial part has solutions that are linear combinations of $\sin(p_x x + p_y y)$ and $\cos(p_x x + p_y y)$, with $p_x^2 + p_y^2 = p^2$. For a universe with $a \propto \tau^\alpha$, the solutions to this equation are of the form $\varepsilon = \tau^\nu \mathsf{Z}_\nu(p\tau)$; $\nu = (1 - 3\alpha)/2$.

Energy and momentum. We perform the variation in Eq. (4.13) for the scenario in question to find the SE tensor associated with the wall motion. The detailed calculation can be found in Appendix A.2. The non-vanishing spatial components are

$$\begin{aligned} T_{ab}(\tau, \boldsymbol{x}) &= -a\sigma\, \Phi_l(z - z_\mathrm{w})\, \eta_{ab} \\ T_{(i3)}(\tau, \boldsymbol{x}) &= -a\sigma\, \Phi_l(z - z_\mathrm{w})\, \epsilon_{,i} \end{aligned} \tag{4.21}$$

where indices $a, b = 0, 1, 2$.

4.2.1 Time-dependent surface tension

Until now, the theory is model-independent in the sense that we have not assumed any particular type of domain wall (or defect, in general). This dependence is encoded in the *constant* surface tension σ and difference in vacuum energies $v = v_+ - v_-$. It is plain to see from Eq. (4.7) that the absence of energy bias removes the surface-tension dependence. But what if the surface tension is not constant?

If we allow the surface tension to vary, $\sigma = \sigma(\tau)$, we need to put this inside of the integral in the Nambu–Goto action in Eq. (4.4). We immediately see that this is equivalent to letting $a^3 \to a^3\sigma$, which amounts to

$$f(\tau) = \frac{3}{a\sigma^{1/3}}\frac{\mathrm{d}a\sigma^{1/3}}{\mathrm{d}\tau} = 3\frac{\dot{a}}{a} + \frac{\dot{\sigma}}{\sigma} = 3\frac{\mathrm{d}\ln a}{\mathrm{d}\tau} + \frac{\mathrm{d}\ln\sigma}{\mathrm{d}\tau} \tag{4.22}$$

in Eq. (4.20). We get

$$\ddot{\varepsilon} + (3\dot{a}/a + \dot{\sigma}/\sigma)\dot{\varepsilon} + p^2\varepsilon = 0. \tag{4.23}$$

This extra term will introduce the model-dependence. As we show in some section[©(next?)] , the surface tension in the thin-wall approximation is

$$\sigma_\mathrm{w} \simeq \int_{\phi_-}^{\phi_+} \mathrm{d}\phi\ \sqrt{2V_\mathrm{eff}(\phi) - 2V_\mathrm{eff}(\phi_\pm)}, \tag{4.24}$$

where $V_\mathrm{eff}(\phi)$ is the effective potential of the scalar field theory.

4.3 TITLE (Symmetron domain walls)

We specify our example even further. The symmetron effective potential in Eq. (3.13) is designed to induce phase transition at conformal time τ_*, or scale factor a_*. Inserting this into Eq. (4.24), we find that the surface tension of a thin symmetron domain wall is

$$\sigma = \sigma_\infty (1-\upsilon)^{3/2}; \quad \upsilon = (a_*/a)^3, \tag{4.25}$$

where σ_∞ is the vacuum surface energy density (Eq. (3.7)).

From here it becomes advantageous to introduce some new, dimensionless variables. We will use $s \equiv \tau/\tau_*$ as our time variable, and $\omega = p\tau_*$ as the eigenvalue, when it comes to that. In a universe with $a = a_* s^\alpha$ we have $\upsilon = s^{-3\alpha}$ and thus

$$\frac{\sigma'}{\sigma} = \frac{\mathrm{d}\ln\sigma}{\mathrm{d}s} = \frac{9\alpha}{2s(s^{3\alpha}-1)}, \tag{4.26}$$

where primes mean derivatives with respect to s. Finally, the equation of motion for the scalar perturbation to the wall normal coordinate is

$$\varepsilon'' + \left(\frac{3\alpha}{s} + 2d(s)\right)\varepsilon' + \omega^2\varepsilon = 0; \quad d(s) \equiv \frac{9\alpha}{4s\,(s^{3\alpha}-1)}. \tag{4.27}$$

4.3.1 Solution in matter-dominated universe

This project only truly experiments in a universe with, and only with, homogeneous matter distribution, i.e. $\alpha = 2$ and $\Omega_{\mathrm{m}0} = 1$. Generalisation of the following to other α should in principle be trivial, but at some point we require $\alpha \geq 1/3$, and so a different analysis would be required for smaller α.

So, restricting our discussion to $\alpha = 2$, we continue with the planar domain wall placed parallel to the xy-plane, spontaneously formed at symmetry break, $s = 1$. Assume an initial perturbation of amplitude ε_* was given to the wall. We consider the solution to Eq. (4.27) that has eigenvalue $\omega = p\tau_*$ and restrict $\max|\mathscr{E}(x,y)| = 1$ for the spatial part. With initial conditions $\varepsilon(s=1) = \varepsilon_*$ and $\varepsilon'(s=1) = 0$, we shall solve

$$\varepsilon'' + \left(\frac{6}{s} + \frac{9}{2s\,(s^6-1)}\right)\varepsilon' + \omega^2\varepsilon = 0 \tag{4.28}$$

analytically in two regimes, and sow these solutions together in the region where they overlap. For notational ease, we write $\varepsilon(s) = \varepsilon_* e(s)$.

Shortly after symmetry breaking. We begin by solving the equation of motion for $s \sim 1$. As our equation has a singularity at $s = 1$, the natural way to go is through a Laurent expansion around this point of the damping term in Eq. (4.28). We find

$$\frac{6}{s} + \frac{9}{s\,(s^6-1)} = \frac{3}{2}(s-1) + \frac{3}{4} + \frac{29}{8}(s-1) - \frac{93}{16}(s-1)^2 + \mathscr{O}((s-1)^3). \tag{4.29}$$

Now $e(s)$ is also subject to an expansion around $s = 1$;

$$e(s) = \Big[1 + c_1(s-1) + c_2(s-1)^2 + c_3(s-1)^3 + \ldots\Big]. \tag{4.30}$$

When put together, we get a polynomial in $(s-1)$ on the left-hand side of Eq. (4.28), for which all coefficients must vanish. We solve the system of equations for $\{c_1, c_2, c_3\}$ and find

$$e^{(\mathrm{I})}(s) = \left[1 - \frac{\omega^2}{5}(s-1)^2 + \frac{\omega^2}{35}(s-1)^3\right] + \mathscr{O}((s-1)^4). \tag{4.31}$$

Adiabatic evolution. The damping term $2d(s) = 9/(2s(s^6-1))$ initially changes extremely rapidly from very large values, before it becomes very small compared to $3a'/a = 6/s$. We expect the solution to quickly approach that of Eq. (4.20) as $s \gg 1$. Said damping term is not completely negligible, however, as it causes a *damping envelope* that is considered much like in the case of a damped harmonic oscillator, writing

$$e^{(\mathrm{III})}(s) \simeq w(s) \cdot \exp\Big\{-\int^s \mathrm{d}t\, d(t)\Big\}. \tag{4.32}$$

Employing this ansatz in the eom gives

$$w'' + \frac{6}{s}w' + \Big(\omega^2 - \theta(s)\Big)w = 0; \quad \theta(s) = d'(s) + d^2(s) + \frac{6}{s}d(s), \tag{4.33}$$

whose solution is $w(s) \simeq s^{-5/2}\mathsf{Z}_{-5/2}(us)$ when the phase shift introduced by $\theta(s)$ is negligible.[3] Now, we find that $\exp\Big\{-\int^s \mathrm{d}t\, d(t)\Big\} = s^{9/2}(s^6-1)^{-3/4} \cdot \text{constant}$. Thus,

$$e^{(\mathrm{III})}(s) \simeq \frac{A\mathsf{J}_{-5/2}(\omega s) + B\mathsf{Y}_{-5/2}(\omega s)}{s^{5/2}} \frac{s^{9/2}}{(s^6-1)^{3/4}}, \tag{4.34}$$

where A and B are constants to be determined.

Complete evolution. We use a computer algebra system, namely *SageMath* [18], to determine A and B from the system of equations

$$\begin{aligned} e^{(\mathrm{I})}(s = s_{\mathrm{sow}}) &= e^{(\mathrm{II})}(s = s_{\mathrm{sow}}), \\ e^{(\mathrm{I})\prime}(s = s_{\mathrm{sow}}) &= e^{(\mathrm{II})\prime}(s = s_{\mathrm{sow}}), \end{aligned} \tag{4.35}$$

⌜maybe put expressions in appendix?⌟ where we choose $s_{\mathrm{sow}} = 1 + \omega^{-1}$, since only subhorizon modes, $\omega \gg 1$, are of interest. Now,

$$\varepsilon(s) = \varepsilon_* \cdot \begin{cases} e^{(\mathrm{I})}(s), & s \le s_{\mathrm{sow}}, \\ e^{(\mathrm{III})}(s), & s \ge s_{\mathrm{sow}}. \end{cases} \tag{4.36}$$

In Fig. 4.1 we demonstrate how this solution looks like for arbitrary ω, in the different steps described above. ⌜Should include solution in the case where surface tension is constant.⌟

[3] In fact, it is possible to show that $\lim_{\omega\to\infty}\Big[\sqrt{\omega^2 - \theta(1+\omega^{-1})} - \omega\Big]/\omega = \sqrt{19}/4 - 1 \approx 0.09$.

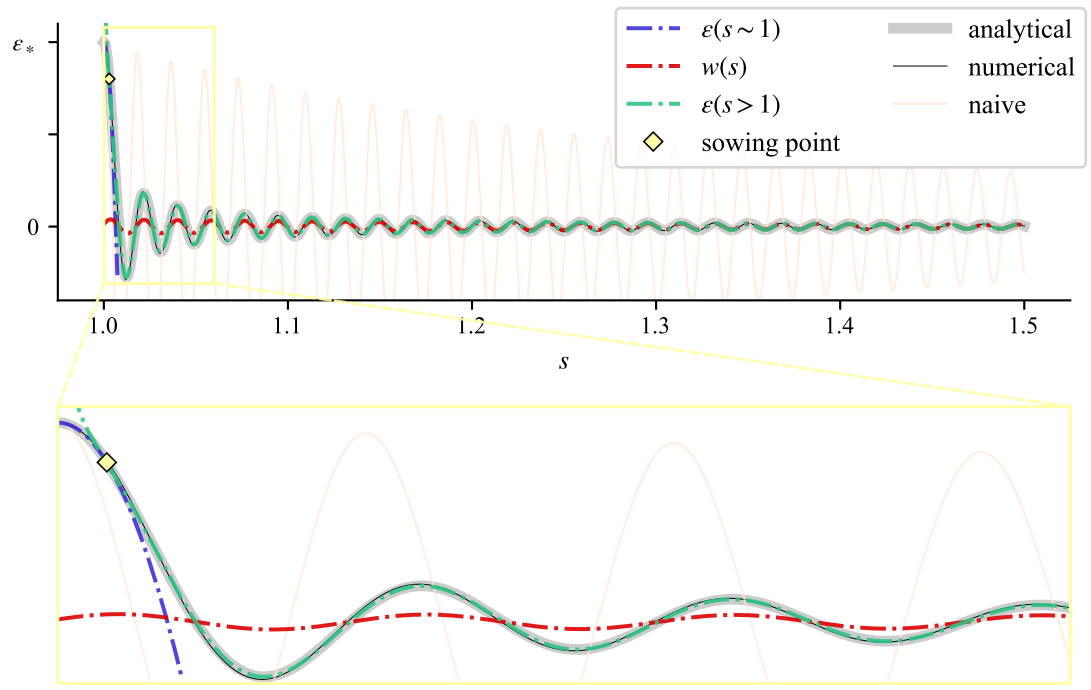

Figure 4.1: Schematic demonstrating how the analytical solution to the eom for $\varepsilon(s)$.

DRAFT

⌜

4.3.2 TITLE (Review)

Figure 4.2: Demonstration of the effect of changing scale parameter $\omega = p\tau_*$.

For the time being, let us assume Eq. (4.36) is a good description of the perturbed symmetron wall. We immediately see that the initial amplitude ε_* can be factored out and does not affect

the evolution. We keep in mind that this parameter is still important for the validity of the eom that requires $\varepsilon_* \ll \tau_*$. The scale parameter $\omega = p\tau_*$ determines the frequency of oscillations. We observe that this result ⌈is completely independent of τ_*.⌋?

Scaling. It turns out that if plotted over the time variable $t_\omega \equiv \omega(s-1) = p(\tau-\tau_*)$, the solution in Eq. (4.36) is ⌈equal up to normalisation in ε_*⌋?

Spatial part

If we for simplicity let $p_y = p$ and impose Dirichlet boundary conditions $\mathscr{E}(y = 0) = \mathscr{E}(y = \tau_*) = 0$, we can write the solution in terms of eigenvalues $p^{(n)} = \pi n/\tau_*$,

$$\epsilon(\tau, y) = \sum_{n=0}^{\infty} \{a_n F_a(s; \pi n) + b_n F_b(s; \pi n)\} \sin(p^{(n)} y), \tag{4.37}$$

where $F_{a,b}(s; \omega^{(n)})$ are the linearly independent solutions to Eq. (4.28).

- Extensions:
  - Superposition of perturbations,
  - Various choices of spatial parts
  - Asymmetron/energy bias — maybe very difficult to combine with time-dependent surface tension

Asymmetron domain walls

Let us have a quick peek at what would happen if introducing asymmetry in the potential. We consider a constant surface tension and vacuum energy densities. In the thin-wall limit, we should be able to use

⌟

4.4 Generation of gravitational waves

⌈In the absence of asymmetry, a domain wall will not produce disturbances in the gravitational field. However, perturbations to the wall position, such as ripples or wiggles, can reveal themselves as tensor perturbations to the background metric. ⌟

Planar domain walls do not themselves produce gravitational radiation. Introducing asymmetry to the system, as we do when adding perturbations, can give rise to non-vanishing stress–energy tensor components in the TT gauge. In this section we present the gravitational-wave calculations in the case of a planar, thin domain wall in a conformally flat universe with expansion rate a.

We neglect back-reaction, that is we assume that the defect does not change the unperturbed background metric. The calculations largely follow Kawasaki and Saikawa [14].

4.4.1 TITLE (Dynamics of gravitational waves in expanding universe)

From Section 2.4.1 we have an expression for $h_{ij}(\tau, \boldsymbol{k})$ in a universe with $a \propto \tau^\alpha$. Consider $\alpha \in \mathbb{Z}$. Assuming homogeneous initial conditions at $\tau_{\text{init}} = \tau_*$, the tensor perturbations are given by Eq. (2.25) and Eq. (2.24) with $n = \alpha - 1$. For convenience, we use a linear polarisation basis (see Section 2.4.2) and the decomposition $\bar{h}_P = H_P^1 + H_P^2$ such that

$$\begin{aligned} H_P^1(\tau, \boldsymbol{k}) &= +\mathsf{S}_n(k\tau) \int_{\tau_*}^{\tau} \mathrm{d}\eta\, \mathsf{C}_n(k\eta) f_P(\eta, \boldsymbol{k}), \\ H_P^2(\tau, \boldsymbol{k}) &= -\mathsf{C}_n(k\tau) \int_{\tau_*}^{\tau} \mathrm{d}\eta\, \mathsf{S}_n(k\eta) f_P(\eta, \boldsymbol{k}). \end{aligned} \tag{4.38}$$

$f_P = 16\pi G_{\text{N}} a T_P^{\text{TT}}/k^2$ contains the TT-projected stress–energy tensor. The conformal time derivative $\dot{\bar{h}} = \dot{H}_P^1 + \dot{H}_P^2$ is given by

$$\begin{aligned} \dot{H}_P^1(\tau, \boldsymbol{k}) &= +k\left[\mathsf{S}_\alpha(k\tau) - n\mathsf{j}_n(k\tau)\right] \int_{\tau_*}^{\tau} \mathrm{d}\eta\, \mathsf{C}_n(k\eta) f_P(\eta, \boldsymbol{k}), \\ \dot{H}_P^2(\tau, \boldsymbol{k}) &= -k\left[\mathsf{C}_\alpha(k\tau) - n\mathsf{y}_n(k\tau)\right] \int_{\tau_*}^{\tau} \mathrm{d}\eta\, \mathsf{S}_n(k\eta) f_P(\eta, \boldsymbol{k}). \end{aligned} \tag{4.39}$$

Note that $\dot{h} = a^{-1}(\dot{\bar{h}} - \dot{a}\bar{h})$ is the conformal time derivative of the gravitational waves.

DRAFT

⌜

4.4.2 Fourier space stress–energy tensor

- Fourier space SE tensor
- TT gauge

From Section 4.2 we found that the SE tensor of a thin domain wall in an expanding universe looks like Eq. (4.21), which for the case of a wall in the xy-plane reduces to

$$\begin{aligned} T_{ab}^{\text{w}}(\tau, \boldsymbol{x}) &= -a(\tau)\sigma(\tau)\Phi_l(z - z_{\text{w}})\,\eta_{ab}, \\ T_{iz}^{\text{w}}(\tau, \boldsymbol{x}) &= -a(\tau)\sigma(\tau)\Phi_l(z - z_{\text{w}})\,\epsilon_{,i}, \end{aligned} \tag{4.40}$$

where $z_{\text{w}} = z_0 + \epsilon(x^a)$ and Φ_l is a Gaussian with standard deviation $l = \delta_{\text{w}}/2$. We go further and look at this quantity in Fourier space:

$$\begin{aligned} T_{ab}^{\text{w}}(\tau, \boldsymbol{k}) &= -a(\tau)\sigma(\tau)\,\eta_{ab}\,\mathscr{D}_{\text{w}}(k_z) \int d^2x\, \mathrm{e}^{-\mathrm{i}k_z\epsilon}\mathrm{e}^{\mathrm{i}(k_x x + k_y y)}, \\ T_{iz}^{\text{w}}(\tau, \boldsymbol{k}) &= -a(\tau)\sigma(\tau)\,\mathscr{D}_{\text{w}}(k_z) \int d^2x\, \epsilon_{,i}\mathrm{e}^{-\mathrm{i}k_z\epsilon}\mathrm{e}^{\mathrm{i}(k_x x + k_y y)}, \end{aligned} \tag{4.41}$$

where $\mathscr{D}_{\mathrm{w}}(k_z) = \exp\!\left\{-\mathrm{i}k_z z_0 - (k_z\delta_{\mathrm{w}})^2/8\right\}$ adjusts for wall width and origin. Let us assume $\epsilon_{,x} = 0$ s.t. $\epsilon(\tau, x, y) = \varepsilon(\tau)\mathscr{E}(y)$ with eigenvalue p^2. Now

$$\underbrace{\int \mathrm{d}y\, \mathrm{e}^{-\mathrm{i}k_z\varepsilon(\tau)\cdot\mathscr{E}(y)}\mathrm{e}^{\mathrm{i}k_y y}}_{I_{\mathrm{s}}} \quad \text{and} \quad \underbrace{\varepsilon(\tau)\int \mathrm{d}y\, \partial_y\mathscr{E}\, \mathrm{e}^{-\mathrm{i}k_z\varepsilon(\tau)\cdot\mathscr{E}(y)}\mathrm{e}^{\mathrm{i}k_y y}}_{I_{\mathrm{a}}} \tag{4.42}$$

are all we need to solve to have a completely analytic expression for $T^{\mathrm{w}}_{ij}(\tau, \boldsymbol{k})$.

Choice of spatial part

It is not obvious what to choose for $\mathscr{E}(y)$. In this project, we started out with $\mathscr{E}(y) = \sin py$, which luckily worked out (though not easily).

The advantage of reducing the problem to spatial dimensions y and z becomes very clear when converting to a linear polarisation basis. We show in appendix X$^{\copyright}_{()}$ that

$$e^{+}_{ij}(\boldsymbol{k}) = \frac{1}{k^2}\begin{pmatrix} k^2 & 0 & 0 \\ 0 & -k_z^2 & k_y k_z \\ 0 & k_y k_z & -k_y^2 \end{pmatrix}_{ij} \quad \wedge \quad e^{\times}_{ij}(\boldsymbol{k}) = \frac{1}{k}\begin{pmatrix} 0 & k_z & -k_y \\ -k_z & 0 & 0 \\ k_y & 0 & 0 \end{pmatrix}_{ij} \tag{4.43}$$

holds for $\boldsymbol{k} = \boldsymbol{k}_{\llcorner} \equiv (0, k_y, k_z)$, which is enforced by the Fourier transform of unity in $T_{ij}(\tau, \boldsymbol{x})$. We observe that $h_{ix} = \delta_{ix}h_{xx}$, so $h_{\times} = 0$. This means we only need $\Lambda_{xx}{}^{ij}T_{ij}$ to get the full h_{ij} from the thin domain wall. We use the projection tensor given in some equation$^{\copyright}_{(\text{notation sec.?})}$ to obtain

$$T^{\mathrm{TT}}_{xx}(\tau, \boldsymbol{k}_{\llcorner}) = \frac{1}{2k^2}\left\{k_y^2 T_{xx} + 2k_y k_z T_{xy}\right\}(\tau, \boldsymbol{k}_{\llcorner}). \tag{4.44}$$

We present in Appendix A the calculation to get an analytical expression for T^{TT}_{xx} with $\mathscr{E}(y) = \sin py$. $-+\times$

blah blah [...] (appendix)

$$\begin{aligned} I_{\mathrm{s}} &= 2\pi\sum_{n\in\mathbb{Z}} \delta(k_y + np)\cdot \mathsf{J}_n(k_z\epsilon_p) \\ I_{\mathrm{a}} &= 2\pi\sum_{n\in\mathbb{Z}} \delta(k_y + np)\cdot \mathsf{J}_n(k_z\epsilon_p)\cdot\frac{np}{k_z} \end{aligned} \tag{4.45}$$

We explore the general behaviour of the non-vanishing modes.

Transverse-traceless gauge

We extract the transverse and traceless part of the SE tensor by use of the projection operator$^{\copyright}_{(\text{early chap.})}$.

$$T^{\mathrm{TT}}_{+} = T^{\mathrm{TT}}_{xx} = \frac{1}{2k^2}\left[k_y^2 T_{xx} + 2k_y k_z T_{xy}\right] \tag{4.46}$$

$$T^{\mathrm{TT}}_{+} = \frac{1}{2k^2}\,\mathcal{T}(\tau, k_x, k_z)\left[k_y^2\mathscr{I}_1 + 2k_y k_z\mathscr{I}_2\right] = -\frac{k_y^2}{2k^2}\,\mathcal{T}(\tau, k_x, k_z)\mathscr{I}_1(\tau, k_y, k_z) \tag{4.47}$$

4.4.3 Examples

How will the domain wall manifest in the gravitational waves, given our equations? Let us have a look at some examples. When $z_0 = 0$, $h_+ = \Re\{h_+\}$.

Both the perturbation scale parameter u *and* the initial amplitude ε_* contribute to the GW signature.

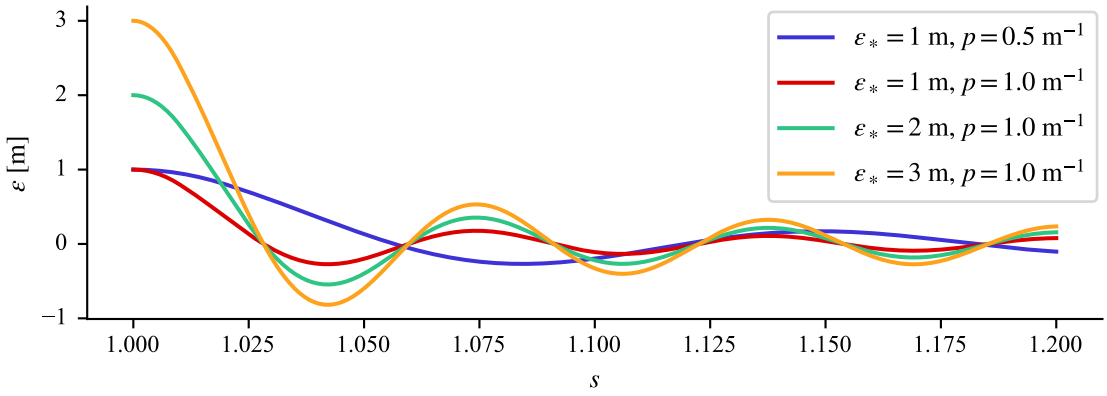

(a) X.

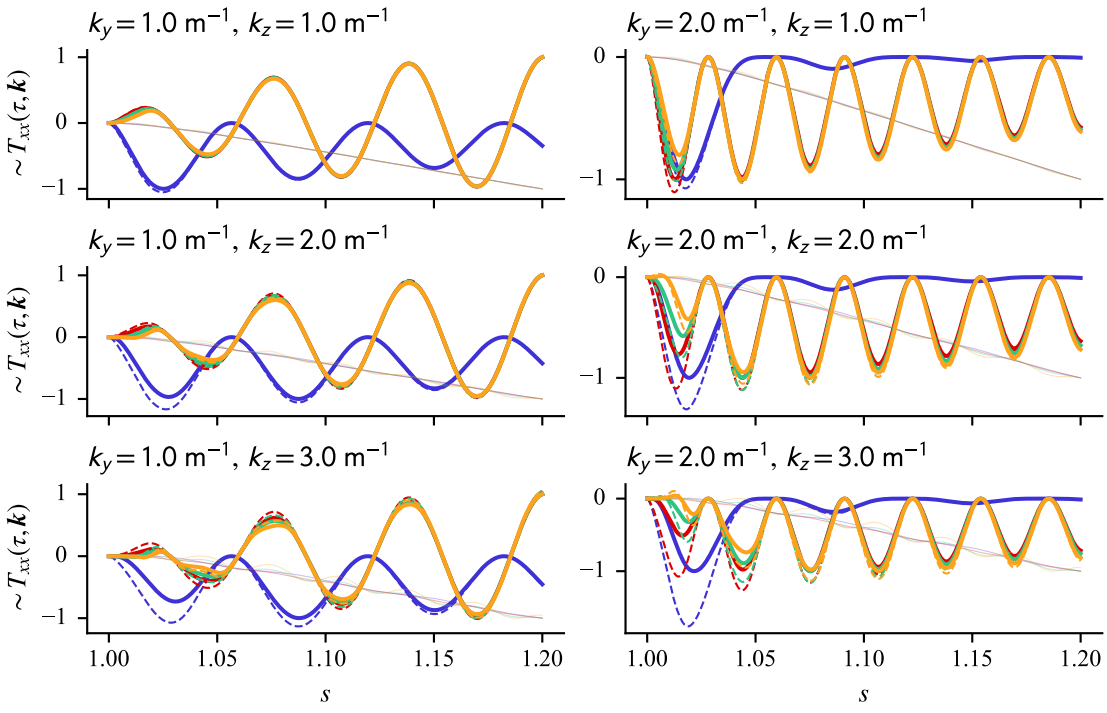

(b) Gravitational waves from ....

Figure 4.3: In units where m $\equiv \tau_*/100$.

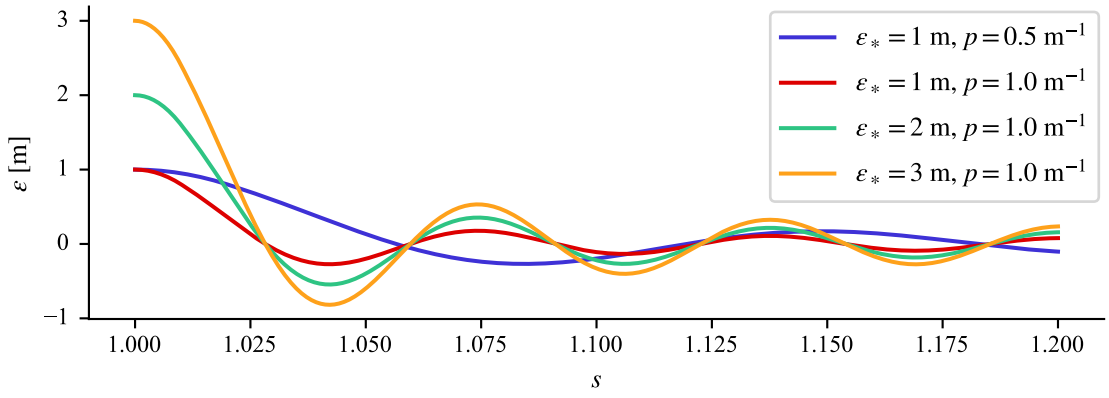

(a) X.

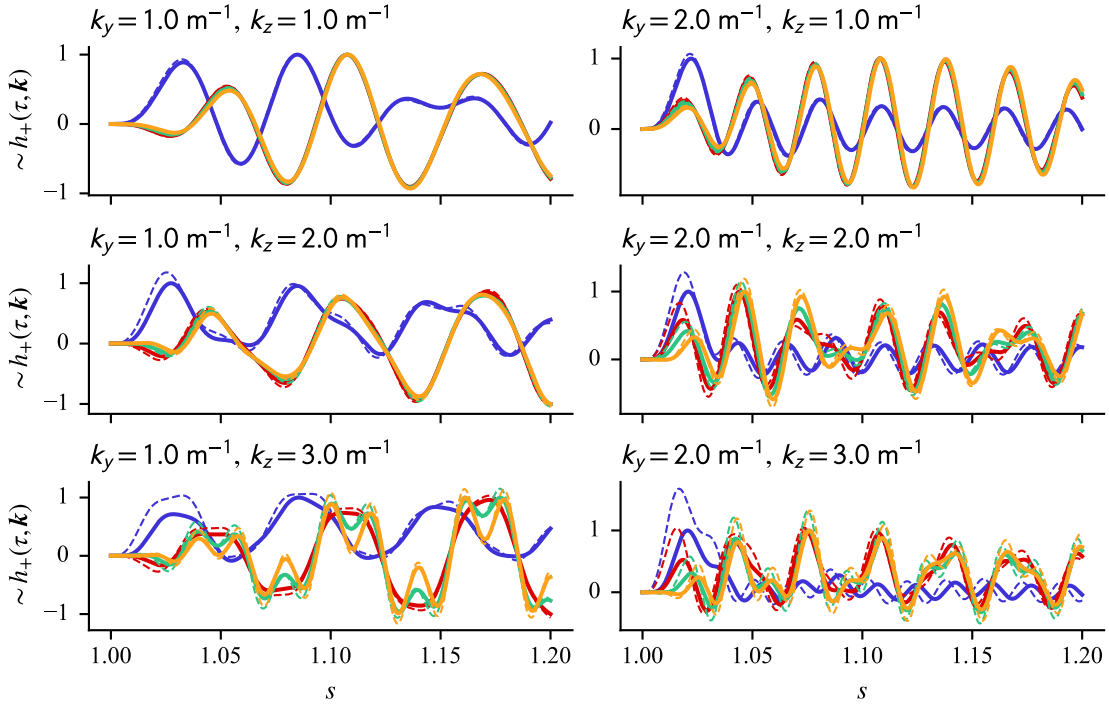

(b) Gravitational waves from ....

Figure 4.4: In units where m $\equiv \tau_*/100$.

Chapter 5

TITLE (Cosmic Phase Transition)

- Testing the framework
- Different theory
- Comment on annihilation?
- First, go through the field description (modified gravity, Symmetron)

Discrete symmetry breakage leads to formation of domain walls. The thin-wall approximation is not suited to describe the dynamics at this stage, and is ⌈certainly not able to tell the whole story.⌋ A Lagrangian that are reflection-invariant in a scalar field theory, and then suddenly is not any more, describes a system that undergoes a phase transition. In the case of $3+1$ dimensions, the system is quickly divided into alternating positive and negative vacuum domains. Separating these are stable domain walls—the newborn soliton solution for the scalar field. During the early stages of formation, a domain wall in theory reduces its thickness from initially infinite to $\sim \delta_\infty = \mu^{-1}$; a source of various problems both simulation-wise and for the theory.

In this chapter we attack the field-theoretical approach to describing the motion of domain walls. We eventually take leave of one spatial dimension, and so the framework also describes strings. Previous work [2] has been done on Minkowski background in the static picture. This analysis assumes a conformally flat, homogeneous and isotropic background, particularly one with scale factor $a \propto \tau^\alpha$. We consider the entire phase transition, i.e. the actual formation of defects, which alters the dynamics in the Nambu–Goto picture. We build up towards simulations of toy scenarios for which we set $\alpha = 2$.

5.1 $\mathbb{Z}_2$ symmetry break

Assume the boson ϕ is responsible for symmtetry break at $a = a_*$, when the energy density of the universe is $\rho = \rho_*$. From Section 3.2.2 we have the (a)symmetron effective potential Eq. (3.13), and the equation of motion for the scalar field $\Box\phi = V_{\text{eff},\phi}$ reads

$$-a^{-2}\left[\ddot{\phi} + 2\mathcal{H}\dot{\phi} - \boldsymbol{\nabla}^2\phi\right] = \lambda\phi^3 + \mu^2(\upsilon - 1)\phi, \tag{5.1}$$

where $\upsilon = \rho_{\text{m}}/(\mu M)^2$. To solve this highly nonlinear equation we evaluate it in the quasistatic and spatially asymptotic limits.

In the rest of the thesis we use the scaled quantities $\chi = \phi/\phi_\infty$, $\phi_\infty = \mu/\sqrt{\lambda}$ and $\chi_\pm = \pm\sqrt{1-\upsilon}$. Prior to SSB, the scalar field solution is trivial, and so we move on to consider χ from

this critical point where the quartic term turns negative and the $\mathbb{Z}_2$ symmetry is spontaneously broken. In the following, we only address the regime where $\rho_{\rm m} < \rho_*$.

5.1.1 Quasistatic limit

We can solve

$$\boldsymbol{\nabla}^2\chi \simeq +\mu^2 \cdot a^2\Big[\chi^2 - \chi_+^2\Big]\chi \tag{5.2}$$

to obtain the solution in the limit where spatial gradient plays a much larger role that time derivatives. For $a = 1$ and $\chi_+ = 1$ the solution is the canonical soliton ⌈from Section 3.1.1⌋?. We consider the well-established extension [see e.g. 17] for the corresponding defect in an expanding universe in combination with adjusting for varying minima [15], namely

$$\chi_{\rm w}(a, z) = \chi_+ \tanh\left(\frac{\chi_+ az}{2L_{\rm C}}\right), \tag{5.3}$$

where $L_{\rm C}$ is the symmetron Compton wavelength.©(chap. 3)

Basic properties. Consider the conventional $\mathbb{Z}_2$ wall from Section 3.1.2. Extrapolated to expanding spacetime, we get

$$\sigma_{\rm w} = \sigma_\infty(1-v)^{3/2} \quad \text{and} \quad a\delta_{\rm w} = \delta_\infty(1-v)^{-1/2} \tag{5.4}$$

as expressions for the comoving thickness $\delta_{\rm w}$ and the surface energy density $\sigma_{\rm w}$, where δ_∞ and σ_∞ are given in Eq. (3.7).

5.1.2 Asymptotic limit

We let $\breve{\chi}$ denote the field value far away from the wall, well inside the domains. Here,

$$\breve{\chi}'' + 2\mathcal{H}\breve{\chi}' = -\mu^2 \cdot a^2\Big[\breve{\chi}^2 + v - 1\Big]\breve{\chi} \tag{5.5}$$

governs the evolution of the field strength. The trivial solution becomes unstable after the phase transition, and the field may fall into any of the two vacua, depending on the phase of the a priori fluctuations. We take a look at one of the minima. The positive minimum, which was zero at PT, goes as $\chi_+ = \sqrt{1-v}$. Now, the rate at which χ_+ moves from its initial value, blows up at the phase transition, but decays rapidly when approaching the limit value. It makes sense to analyse the equation in the **(I)** non-adiabatic and **(II)** adiabatic regimes separately.

The non-adiabatic regime **(I)** is a short window around PT in which the effective potential changes faster that what the dynamics of the scalar field allow. That is to say, the asymptotic field value $\breve{\chi}$ cannot possibly hope to follow the system's actual minima $\chi_\pm$. When the scalar catches up, the effective potential changes slower than the field in what we call the adiabatic regime **(II)**. What happens is that the field rolls towards the minimum and begins to oscillate around it whilst following its slow drift. The oscillation amplitude is decided by the initial conditions of the field.

We know that oscillations in the scalar field can themselves produce gravitational waves [14]. Ideally we would get rid of them completely to not contaminate the ⌈kinky gravitational waves.⌋◡ In addition, these oscillations will to some extent affect the surface tension and thickness of the domain wall. This will in turn alter the equations for ϵ and h_{ij} from the NG theory, making them analytically unsolvable. So we should avoid large oscillations in the scalar field at ⌈any⌋◡ cost.

How to go about this is explained in detail in Appendix B. We use the result to put new boundary conditions on the quasistatic equation Eq. (5.2).

5.2 Dynamic modelling

The list of assumptions and terms starting with "quasi" has become uncomfortably long. Most of these have been tested before or are otherwise motivated by similar established phenomena in Minkowski space. We want to test how the thin-wall NG dynamics associates with the field-theoretically formulated dynamics of a cosmic phase transition, explicitly in a generic spacetime. Cosmological contexts seldom care about spacetimes other than FLRW. The effect of curvature is insignificant in the Friedmann equations, thus irrelevant in *our* universe, and we can safely assume (conformal) flatness. ⌜Bold statement, no?⌟

5.3 `gwasevolution` (On the lattice?)

As test bed for our theory we use `gwasevolution` [6], an extended version of the massively parallelised N-body relativistic code `gevolution` [1]. LATfield2 [8] is used as backend to this and was originally blah blah [...]

⌜Possibly appendix about HPC⌟

The general setup is a three-dimensional box of equal side lengths $L_\#$ in Mpc/h_0 on a lattice of $N_\#^3$ points, giving a spatial resolution of $\Delta_\# = L_\#/N_\#$.

The mapping from code configuration space to comoving coordinates is:

$$\begin{aligned} \boldsymbol{x} &= \mathtt{x}_{\mathtt{i},\mathtt{j},\mathtt{k}} \cdot \Delta_\#, \\ (x, y, z) &= (\mathtt{i}, \mathtt{j}, \mathtt{k}) \cdot \Delta_\#. \end{aligned} \tag{5.6}$$

Meanwhile, the corresponding mapping in Fourier space is given in terms of the fundamental frequency $k_\# = 2\pi/L_\#$:

$$\begin{aligned} \boldsymbol{k} &= \mathtt{k}_{\mathtt{u},\mathtt{v},\mathtt{w}} \cdot k_\#, \\ (k_x, k_y, k_z) &= (\mathtt{u}, \mathtt{v}, \mathtt{w}) \cdot k_\#. \end{aligned} \tag{5.7}$$

⌜comment about hermitian symmetry?⌟

5.3.1 Periodic boundaries

The simulation box is a torus as it has periodic boundaries—a common choice for cosmological simulations.

- Dirac comb: $\text{Ш}_{L_\#}(z) = \frac{1}{L_\#}\text{Ш}(z/L_\#)$

5.3.2 Initial configuration

To accurately compare the soliton's evolution with the NG prediction, it is essential to begin with an initial configuration closely approximating the exact solution to the equations of the full field theory. Without this, any deviations from the NG dynamics might simply result from inaccuracies in the initial setup.

That said, we do not actually have these exact solutions in curved spacetime. However, with sufficient tweaking, the setup should be close enough to blah blah [...]

The purpose of the simulations is to test the applicability of the thin-wall approximation for the wall evolution (Eq. (4.36)) and the corresponding gravitational waves (Section 4.4).

Therefore, the simulation setup imitates a toy model, not a realistic system. To create this idealised cosmological scenario we initialise the simulation box as described below.

We assume wall profiles of the form

$$\chi_{\rm w}(a_{\rm init}, z - z_{\rm w}) = \breve{\chi} \tanh\left(\frac{a\breve{\chi}}{2L_{\rm C}}(z - z_{\rm w})\right)\Big|_{a=a_{\rm init}}, \tag{5.8a}$$

$$q_{\rm w}(a_{\rm init}, z - z_{\rm w}) = a^2 \frac{{\rm d}\chi_{\rm w}}{{\rm d}\tau}\Big|_{a=a_{\rm init}}, \tag{5.8b}$$

where a, $\breve{\chi}$ and $z_{\rm w}$ generally depends on time and $z_{\rm w}$ on space. Note with $\breve{\chi} = \chi_+$ we get the familiar quasistatic formula in Eq. (5.3). For more details we refer to Appendix B.

(achi) In an FLRW universe a (semi-)stable Symmetron domain wall is approximated Eq. (5.3) (or Eq. (B.8)). To preserve boundary conditions, there needs to be at least two walls present. We choose to place the wall of interest at $z_0 = L_\#/2$, and its counterpart—the anti-wall—at $\bar{z}_0 = 0$, both aligned with the xy-plane.

Now say we add a displacement $\epsilon = \epsilon(\tau, x, y)$ to the middle wall. Assuming sufficient spatial separation, the system of defects is given by

$$\chi(a, z) = \prod_{n=-\infty}^{\infty} \chi_{\rm w}(a, z - z_{\rm w}^n) \prod_{m=-\infty}^{\infty} \bar{\chi}_{\rm w}(a, z - \bar{z}_{\rm w}^m), \tag{5.9}$$

where

$$z_{\rm w}^n = z_0 + \epsilon + nL_\# \quad \text{and} \quad \bar{z}_{\rm w}^m = \bar{z}_0 + mL_\#. \tag{5.10}$$

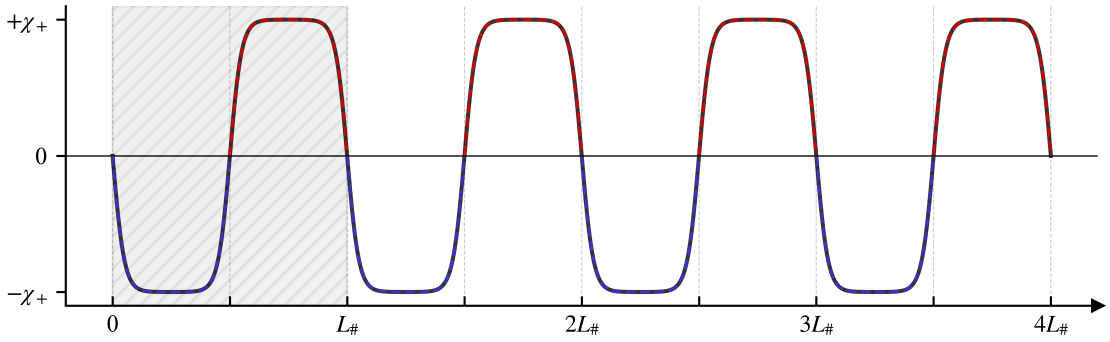

Figure 5.1: Demonstration of the periodicity of $\chi(a_{\rm init}, z)$ on the lattice.

(aq) Setting the initial conditions on the field $q = a^2\dot{\chi}$ is a matter of algebra. The expression is cleanest when $\dot{z}_{\rm w} = \dot{\epsilon} = 0$, i.e. for $a_{\rm init} = a_*$.

Initial time. We need to be careful when choosing the exact redshift to initiate the simulation. Clearly, the conventional expression Eq. (5.3) does not work if we set initial redshift $\mathfrak{z}_{\rm init} = \mathfrak{z}_*$. Initiating only a few time steps later allows us to use this after all, but we need to make sure the wall and anti-wall do not collide. Whether this is the case depends on several parameters. Some sets of initial conditions will induce large fifth force oscillations, and we should try to avoid this.

Using the tweaked initial conditions on the asymptotic fields as boundary conditions on the quasistatic field in Eq. (B.8) opens for the possibility of initialising as close to phase transition as we want.

We see that $\check{\chi} \to \chi_+$ after some time, and so another strategy to reduce oscillations is to initialise *after* this non-adiabatic phase. The draw-back is that we might lose important information about the source of the gravitational waves.

DRAFT

⌜

Stress–energy tensor

We have the SE tensor $T_{\mu\nu}(\tau, \boldsymbol{x}) = \sum_n T^{\mathrm{w}(n)}_{\mu\nu}(\tau, \boldsymbol{x}) + \sum_m \overline{T}^{\mathrm{w}(m)}_{\mu\nu}(\tau, \boldsymbol{x})$, which we can write as (see Section 4.4.2)

$$\begin{aligned} T_{ab}(\tau, \boldsymbol{x}) &= -a\sigma\eta_{ab} \sum_n \left[\Phi_{\delta_{\mathrm{w}}/2}(z - z^n_{\mathrm{w}}) + \Phi_{\delta_{\mathrm{w}}/2}(z - \overline{z}^n_{\mathrm{w}})\right], \\ T_{iz}(\tau, \boldsymbol{x}) &= -a\sigma \sum_n \left[\Phi_{\delta_{\mathrm{w}}/2}(z - z^n_{\mathrm{w}})\partial_i z^n_{\mathrm{w}} + \cancel{\Phi_{\delta_{\mathrm{w}}/2}(z - \overline{z}^n_{\mathrm{w}})\partial_i \overline{z}^n_{\mathrm{w}}}\right], \end{aligned} \tag{5.11}$$

where z^n_{w} and $\overline{z}^n_{\mathrm{w}}$ are given in Eq. (5.10).

Going to Fourier space, we have

$$\begin{aligned} T_{ab}(\tau, \boldsymbol{k}) &= -a\sigma\eta_{ab} \sum_n \left[\mathscr{D}^n_{\mathrm{w}}(\tau, k_z) \int d^2x\, \mathrm{e}^{-\mathrm{i}k_z\epsilon}\mathrm{e}^{\mathrm{i}(k_x x + k_y y)} + \overline{\mathscr{D}}^n_{\mathrm{w}}(\tau, k_z)\delta(k_x)\delta(k_y)\right], \\ T_{iz}(\tau, \boldsymbol{k}) &= -a\sigma \sum_n \mathscr{D}^n_{\mathrm{w}}(\tau, k_z) \int d^2x\, \epsilon_{,i}\mathrm{e}^{-\mathrm{i}k_z\epsilon}\mathrm{e}^{\mathrm{i}(k_x x + k_y y)}, \end{aligned} \tag{5.12}$$

where $\mathscr{D}^n_{\mathrm{w}} = \mathrm{e}^{-\mathrm{i}k_z L_\#/2} \cdot \overline{\mathscr{D}}^n_{\mathrm{w}}$ and $\overline{\mathscr{D}}^n_{\mathrm{w}} = \exp\left\{-\mathrm{i}k_z n L_\# - (k_z\delta_{\mathrm{w}}(\tau))^2/8\right\}$.

Now, inserting $\epsilon = \varepsilon(\tau)\sin py$ we get

$$T_{xx}(\tau, \boldsymbol{k}) = \tag{5.13}$$

I think I messed it up; should I go through the Dirac comb directly?

5.3.3 Discrete Fourier space

blah blah [...]

$h_{ij}(\eta, \boldsymbol{k}) = \Lambda_{ijkl}(\boldsymbol{k})h_{kl}(\eta, \boldsymbol{k})$ where $\boldsymbol{k}$ is *not* defined $\boldsymbol{k} = 2\pi(\mathrm{u}, \mathrm{v}, \mathrm{w})/L$

blah blah [...]

$$T^{\mathrm{ww}}_{ij}(\tau, \boldsymbol{x}) = T^{\mathrm{w}}_{ij}(\tau, \boldsymbol{x}) + \overline{T}^{\mathrm{w}}_{ij}(\tau, \boldsymbol{x}) \tag{5.14}$$

$$T_{ij}(\tau, \boldsymbol{x}) = \sum_n^\infty \delta(\boldsymbol{x}\cdot\hat{\boldsymbol{z}} - nL)T^{\mathrm{ww}}_{ij}(\tau, \boldsymbol{x}) \tag{5.15}$$

$$T_{ij}(\tau, \boldsymbol{x}) = \sum_n^\infty T^{\mathrm{w}}_{ij}(\tau, \boldsymbol{x} - \hat{\boldsymbol{z}}z^n_{\mathrm{w}}) + \sum_m^\infty \overline{T}^{\mathrm{w}}_{ij}(\tau, \boldsymbol{x} - \hat{\boldsymbol{z}}\overline{z}^m_{\mathrm{w}}) \tag{5.16}$$

$$T_{ij}(\tau, \boldsymbol{x}) = \sum_{n}^{\infty} \delta(\boldsymbol{x} \cdot \hat{\boldsymbol{z}} - z_{\mathrm{w}}^{n}) T_{ij}^{\mathrm{w}}(\tau, \boldsymbol{x}) + \sum_{m}^{\infty} \delta(\boldsymbol{x} \cdot \hat{\boldsymbol{z}} - \overline{z}_{\mathrm{w}}^{m}) \overline{T}_{ij}^{\mathrm{w}}(\tau, \boldsymbol{x}) \tag{5.17}$$

The Fourier-space stress–energy tensor becomes

$$T_{ij} = \tag{5.18}$$

5.3.4 TITLE (Options/parameters)

[We now turn to the details of the simulations we are to perform. For starters, we provide options and compiler flags to make certain that fields χ and h_{ij} are computed.]

Numerics. There are choices to be made concerning temporal and spatial resolution, and what integration method to use. Of solvers, there are a handful to choose from, for instance Leap-Frog or fourth order Runge-Kutta. The spatial resolution $\Delta_{\#} = L_{\#}/N_{\#}$ is set by the users choice of box side length $L_{\#}$ in Mpc$/h_0$ and the number of grid points $N_{\#}$ in each direction. The temporal resolution*s* vary for some field updates. They are controlled by the *Courant factors*

$$C_{\mathrm{f}} = v_{\mathrm{g}} \Delta\tau / \Delta_{\#} \tag{5.19}$$

where blah blah [...]

[L and $\vartheta_{\mathrm{init}}$ difficult to place in category.]

Physics. More exciting are the parameters that directly relates to our theoretical setup and cosmological scenarios.

Asymmetron parameters. The code takes the phenomenological parameters $\mathrm{As}_* = \{a_*, \xi_*, \beta_+, \beta_-\}$ and maps them to Lagrangian parameters $\mathrm{As}_{\mathcal{L}} = \{M, \mu, \lambda, \kappa\}$ as described in some section or appendix$^{\copyright}_{()}$.

Perturbation parameters. We added some options to the initialisation-part of the code so to easily create the idealised scenario we want. It has options for this kind of perturbation in the z-direction:

$$\epsilon = \varepsilon(\tau)\, \mathrm{tri}\left\{p_x x + p_y y\right\}; \quad \mathrm{tri} \in \{\sin, \cos\}, \tag{5.20}$$

for which the user can provide initial amplitude ε_* and perturbation scale in terms of scaled, integer wavenumbers $m_{\mathtt{i,j}} = p_{x,y}/k_{\#}$.

We introduce a "curvature" parameter $\Upsilon^{\sim} = 100 m_{\mathtt{j}} \epsilon / L_{\#}$ which will be useful for later discussion.

We need to be careful blah blah [...]

5.4 Simulation setups

PHANTOM PARAGRAPH: SIMULATION DETAILS

Below, we describe the reasoning behind the choice of parameters. As a starting point, we consider the fiducial set of symmetron parameters $a_* = 0.33$, $\xi_* = 3.33 \times 10^{-4}$ and $\beta_* = 1$, following Christiansen [5]. This gives Compton wavelength $L_C \simeq 1\ \mathrm{Mpc}/h_0$ and asymptotic wall thickness $\delta_\infty \simeq \sqrt{2}\ \mathrm{Mpc}/h_0$.

Simulation box

We use a comoving simulation box size that is comparable to the size of the universe—order $\mathcal{O}(\mathrm{Gpc}/h_0)$—so that $\delta_w \ll L_\#$ and the separation between the walls is $\sim L_\#/2$. If we want to resolve the Compton wavelength, this requires $N_\# \geq L_\#/L_C \gtrsim L\ [\mathrm{Mpc}/h_0]$. However, since we are modelling the formation, the walls will blah blah [...]

Initial configuration

The normal quasistatic tanh-profile (Eq. (5.3)) approximates the initial configuration to $\breve{\chi}_* \to 0$ and $\breve{\chi}'_* \to \infty$, which does not actually work out. With the analysis in Section 5.1.2 we can impose suitable initial conditions so that the field rolls into the minima in the most effective way. We need to keep in mind that this affects the surface tension and wall width.

Nature of wall perturbation

We choose to only perturb one wall so that the time of collision between propagating gravitational waves is at $\tau_{\mathrm{init}} + L_\#/2$.[1] We would like $\varepsilon_* \ll L_\#/2$, but simply by looking at Fig. 4.1 we can assume that this would require a very high spatial resolution. As a result, we choose to exaggerate the initial perturbation amplitude and risk higher-order effects.

5.4.1 Catalogue

Every simulation used a 4th order Runge-Kutta solver blah blah [...]

⌜Some extra simulations for convergence testing!⌟

[1] Perturbing both walls would give collision time $\tau_{\mathrm{init}} + L_\#/4$.

Wall–anti-wall simulations

	0	1	2	3	4	5	6	7
Symmetron parameters								
a_*	0.33	0.33	0.33	0.33	0.33	0.33	0.33	0.33
$\xi_* \times 10^4$	3.33	3.33	3.33	3.33	3.33	3.33	1.00	3.33
β_*	1	1	1	1	1	1	1	1
Perturbation parameters ($\varepsilon_* \sin(p_y y)$)								
$\varepsilon_*/L_\#$	0.00	0.08	0.12	0.08	0.08	0.06	0.08	0.08
$p_y/k_\#$	–	2	2	2	2	3	2	2
$\Upsilon_*^\sim$	0	16	24	16	16	18	16	16
Simulation box								
$L_\#$ [Mpc/h_0]	1024	1024	1024	1024	1400	1024	1024	1024
$N_\#$	768	768	768	900	768	960	768	768
Initial configuration								
$\mathfrak{z}_{\text{init}}$	2.00	2.00	2.00	2.00	2.02	2.00	2.00	2.02
$\check{\chi}_{\text{init}}$	-	-	-	-	-	-	-	-
q_{init}	-	-	-	-	-	-	-	-
Numerics								
C_{f}	0.2	0.2	0.2	0.2	0.2	0.2	0.2	0.2
C_{f}					0.2			

Table 5.1: Details about each simulation addressed in Part III. Each simulation is labelled 0 – 7. See Section 5.3 for description of parameters. ⌜Should maybe give fiducial set of parameters (sim. 1) and only give deviations from this.⌟

Part III

Findings

Chapter 6

TITLE (Toy Model Trials)

Title: ***Simulative Insights; Toy Model Trials; Synthetic Experiments;***

This chapter provides simulative insights to our theoretical framework. We both present and discuss results from Table 5.1, and compare this to the theory. The analysis is split into three parts: In Section 6.1 we study the background evolution through box-averaged scalar quantities. Less primitive analysis proceeds in Section 6.2 where the domain wall dynamics of the two theories is compared. Finally, in Section 6.3 we look at what sort of gravitational waves we expect from this phenomenon.

6.1 Background evolution / Symmetron field

In the simplest case where there are no walls present, and the scalar field takes the same value everywhere, the evolution is described solely by Eq. (5.5). In this case, we expect there to be good correspondence between theory and simulation. We found that the optimal path for the symmetron to minimise oscillations occurs if initial conditions are given by Eq. (B.7).

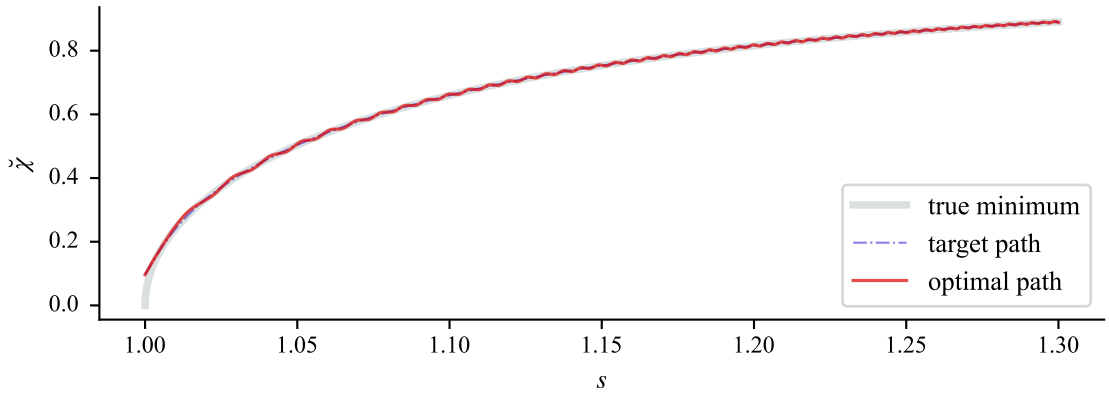

Figure 6.1: The evolution of the symmetron field in the asymptotic limit. The symmetron parameters are the fiducial ones. Not finished plot.

The symmetron field χ (`achi` in the code) will at SSB roll into either minima, depending on the sign of the field right before it happens. The strength of the oscillations around the true minima depend on both the initial field value and its time derivative.

We see in Section 6.1 a handful of background quantities from simulations X, Y and Z.

Figure 6.2: Background quantities.

6.1.1 TITLE (Discussion)

In the absence of topological defects, we see near on perfect correspondence between predicted and simulated scalar field $\check{\chi}$. Presence of walls messes with the maximum field value, due to the "bump" in the profile, but we see from the average squared field value that the overall oscillations are very close to what we expect. ⌜Repeated?⌟

6.2 Domain wall dynamics

Ignore the anti-wall the box's boundaries. Simulation-wise, the wall's position is tracked by the minimum value of $|\chi|$, i.e. the z-coordinate at which the field is closest to zero. We keep in mind that we do not expect a perfect match between the simulated and analytical wall perturbation, mostly because the analytical equations are only valid for perturbations of leading order. A more tangible way to look at is to consider the unit normal vector n^μ that we put along the z-axis; just by looking at the simulations (Fig. 6.3a), we can see that this is clearly not the case, at least close to phase transition.

We reduce the problem from three dimensions to two with cylindrical symmetry, and then again to one dimension by considering a suitable slice in the y-direction and taking the coordinate of the minimal absolute value of the scalar field χ. An example of the two-dimensional perspective is shown in Fig. 6.3a. This picture is more or less the same for all simulations, at least when comparing by-eye.

⌈We see that the quasistatic tanh-solution varies in applicability as it occurs "bumps" around each wall after some time.⌋

The simulated wall position graph is not perfectly overlapping with the analytical one. Simulated walls show a tendency to evolve slower, at least initially, manifesting in a phase difference between $\varepsilon(\tau)$ from simulation and thin-wall approximation. ⌈If not due to numerical

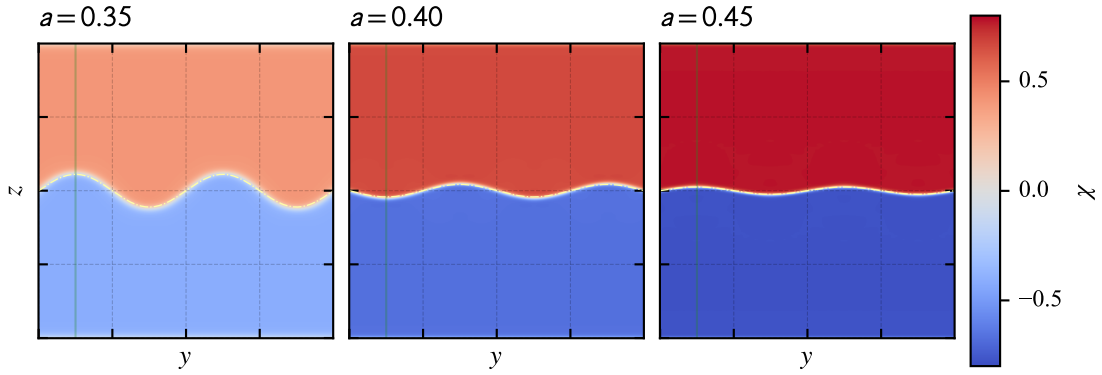

(a) The domain wall evolution in two dimensions. We indicate the aforementioned slice with a green vertical line.

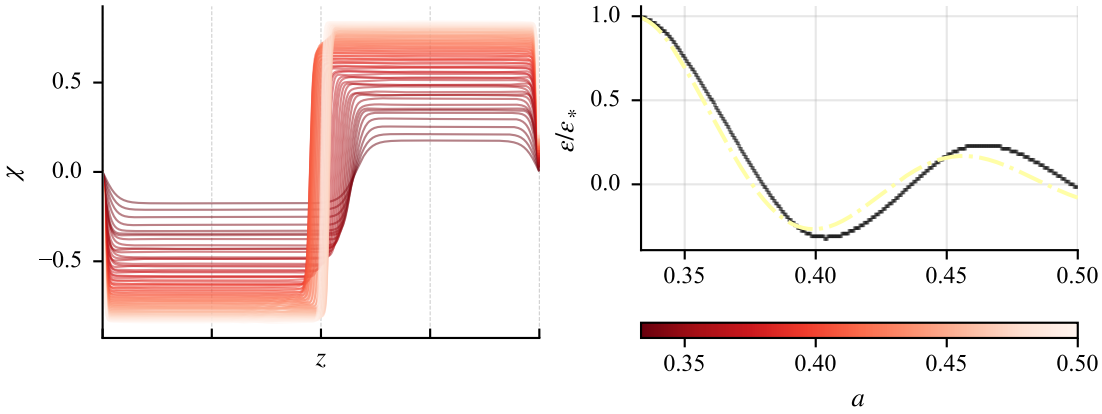

(b) *Left panel:* The scalar field value along y-coordinate XXX at different redshifts. *Right panel:* The wall coordinate as function of time. Note that the colour bar share the same axis as the blah blah [. . .] .

Figure 6.3: Demonstration of results from simulation 1.

error, this is necessarily either a consequence of the field-like description or possibly another damping term in the eom for ε. In the latter scenario, one could guess that the expression for the surface tension is not flawless (something else would insinuate that the expansion term is wrong, which is not the case.) With better spatial resolution, there was no improvement for this part. Initialising simulations even closer to symmetry break enhanced oscillations and increased the phase difference. Increasing the box size—and scaling all parameters thereafter—did not have any effect in this matter. Old analysis, needs to be updated.

We saw that initial amplitude actually did matter in simulations, cf. simulation 1 vs. 2. The thin-wall approximation does not say this, however, in fact it says the opposite; the EOM is scale invariant, and thus unchanged by translations. It is therefore hard to argue that this motion is possible to reproduce by adjusting terms in the EoM.

In Fig. 6.4 we show the difference between the NG prediction, which for $e = \varepsilon/\varepsilon_*$ vs. $t_\omega = \omega(s-1)$ is the same for each simulation, and the field theory. Simulations with similar perturbation setup (cf. 1, 2, 4, 7) but different box parameters gives the similar wall evolution. Note that there is a bump in the simulations with larger scalar field oscillations (4 & 7). Larger initial amplitude (2) increases the difference, as does larger scale parameter (5). This might indicate that the deviation is due to higher-order effects and the linearised analysis fails.

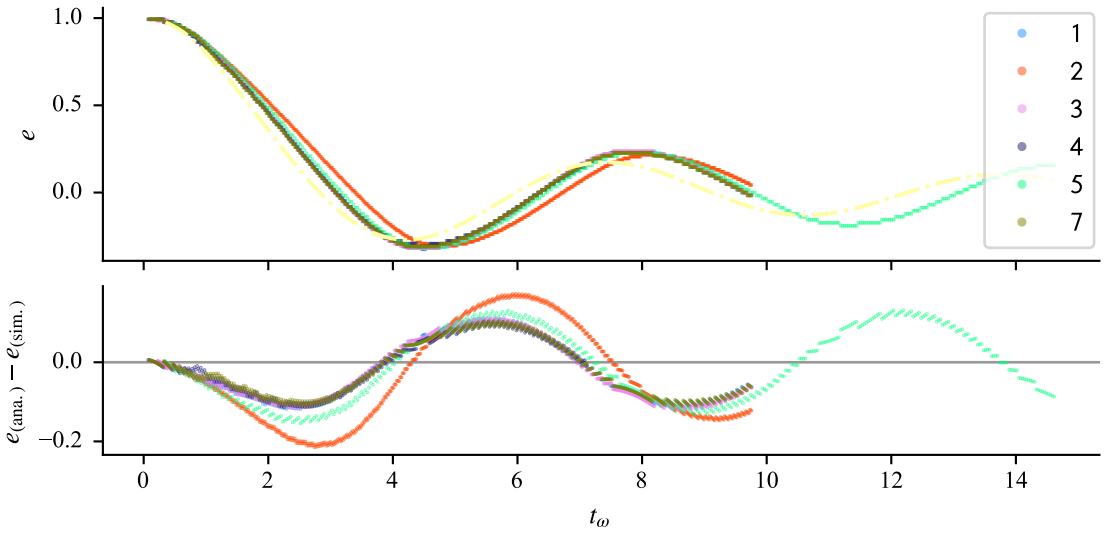

Figure 6.4: The absolute difference between the wall position from calculations and simulations as functions of time.

6.2.1 Adjusting the equation of motion

We take a closer look at the wall evolution in one particular simulation. We discussed the effect of changing the damping term in the equation of motion for blah blah [...] ⌜Study effect of changing damping term.⌟

Figure 6.5: The wall position as depicted by ....

6.2.2 TITLE (Discussion)

Minimising oscillations does not seem to affect the wall evolution particularly. This can be seen by comparing simulations 1, 3, 4 and 7 which all have the same relative initial amplitude, but different levels of oscillations. However, changing the *curvature* of the wall, seems to change the overall behaviour of the wall. In particular, increasing the parameter $\Upsilon_*^{\sim}$ from 16 to 18 (sim. 3) or 24 (sim. 5). We use this as a naive quantification of the badness of the eom for ε; the larger amplitude, the more likely we are to see higher-order effects, and the larger wavenumber, the farther we are from the wall normal coordinate $n^\mu \propto \delta^{\mu z}$. I suppose it is also fair to assume some inter-kink forces or perhaps intra-kink forces could contribute to the equation of motion. It would have been interesting to solve the actual eom for the wall normal coordinate and see if we could come closer to the simulated result. ⌜Repeated argument...⌟

We notice that higher levels of scalar field fluctuations (4 & 7) corresponds to simulations where the wall evolution is ⌈discontinuous⌋◡ in the very beginning. This is apparently not affecting the motion later. The two simulations in question are also characterised by initialisation closer to SSB, a feature that can technically be source of *both* of these phenomena.

6.3 TITLE (Gravitational waves)

The gravitational waves from the NG motion are given by a complicated expression. We have not been able to obtain the corresponding expression in configuration, neither have we found a way to present summary statistics from it.

About the results in general. A few take-aways from the results in all is listed below.

- Zero walls or unperturbed walls produce no GWs.
- The predicted periodicity in k_y agrees with simulations.
- There is definitely a signature of the perturbation in some GW modes.
- Larger scalar field oscillations correspond to noisier GW modes.
- There is a subtlety to the computation of the semi-analytical prediction which shows sensitivity to blah blah [...]

We begin by having a look at the energy density of the gravitational waves, which is obtained through the average conformal time derivative of the *real space* tensor perturbations [14],

$$\rho_{\rm gw} = \frac{1}{32\pi G_{\rm N} a^2(\tau)} \left\langle \dot{h}^{ij}(\tau, \boldsymbol{x}) \dot{h}_{ij}(\tau, \boldsymbol{x}) \right\rangle_{\rm box} = \frac{1}{32\pi G_{\rm N} a^2(\tau)} \frac{1}{N_{\#}^3} \sum_{\mathtt{ijk}} \sum_{ij} \left[\dot{h}_{ij}(\tau, \mathbf{x}_{\mathtt{i,j,k}}) \right]^2. \quad (6.1)$$

⌈In Fig. 6.6 we plot the outcome in two different spaces.⌋◡

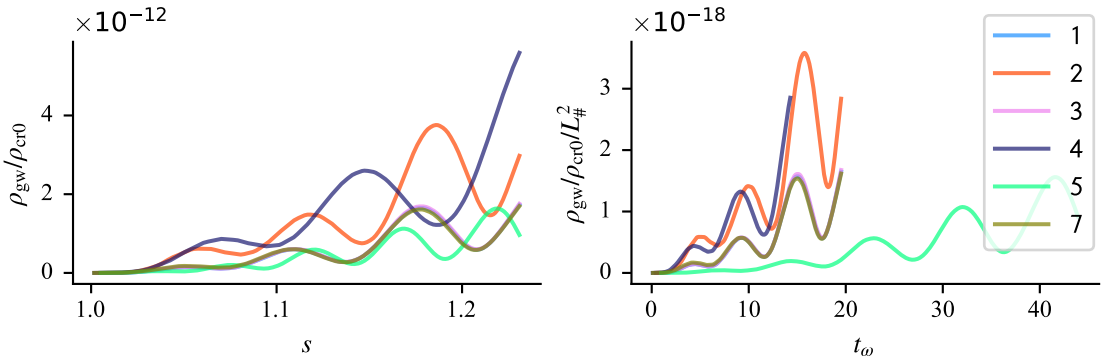

Figure 6.6: The box-averaged ... ⌈FIX PLOT⌋

- Summary statistics! We can focus more on the domain wall dynamics.
- Comment about real/imaginary/absolute value.
- Comment on how the semi-analytical result was obtained (*Numpy*'s `cumtrapz`)

- Looks like $k_z < k_y$ does not carry much information, but I believe that makes sense. They should not be "kinky" here, but free.
- Real component looks generally more messy, might be due to not perfect spatial part?

6.3.1 TITLE (About the comparison)

From simulations, we extract the xx-component of the Fourier-space tensor perturbation, $\mathrm{h}_{xx}(\tau, \mathbf{k})$. We start by checking that $2\mathrm{h}_{xx}^2 = \sum_{ij} \mathrm{h}_{ij}^2$ and conclude that $\mathrm{h}_+ = \mathrm{h}_{xx}$ and $\mathrm{h}_\times = 0$.

One clearly sees characteristics in some tensor modes that definitely has to do with the wall perturbation. However, the correspondence is not obvious in for all modes, the real component and blah blah [...]

6.3.2 Changing the input to the expression

- Adding ingredients to expression for h_{ij} $\rightsquigarrow$ Separate effects
  - Changing ϵ: Changes the "phase"
  - Changing σ: Introduces more small oscillations
  - Changing l (thickness): Even more of the small oscillations

Chapter 7

TITLE (Ifs, buts and maybes)

It is assumed in this chapter that the ⌈theoretical framework checks out.⌋ What would that mean? And how is it applicable to realistic cosmological scenarios? We dedicate this chapter to suggestions for improvements and implications. In the last section we discuss what simulative experiments we would have performed had we more time.

- insert sensible parameters
- propose different spatial parts

Maybe for large scales, scalar field fluctuations contribute a lot? They should peak at the frequency corresponding to the mass scale $m = \sqrt{2}\mu\sqrt{1-v}$*?*

7.1 Limitations and possibilities

Let us review the equations this thin-wall approximation is built on. We want everything up to the Fourier SE tensor to be analytically solvable, at least to some level that resembles the actual situation, like when using $\sigma \propto (1-v)^{3/2}$ in this project. ⌈The behaviour is recognisable at this stage.⌋ Okay, so far, so good. We found that for a two-dimensional topological defect in a conformally flat spacetime, we have the SE tensor $\chi\psi$

$$T_{\mu\nu} = \delta_{\mu\nu}\chi_n\psi\psi \tag{7.1}$$

(z-plane)

Draw-backs. We have not been able to take the tensor analysis back to configuration space.

7.2 Superpositions

- Adding propagating waves on torus
- What would happen if there were two such perturbations? or several pert. walls?

7.3 Improvements

Generalisation: A very natural and possibly straight-forward generalisation would be to let α be a more-or-less free parameter. It should also not be too much work to consider arbitrary dimensions.

Beyond linear perturbation: It would be interesting to solve the eom for the actual wall normal coordinate.

Asymmetron: Adjusting the vacuum energy densities and subsequently the surface tension, in addition to adding an energy bias in the thin-wall approximation, one should be able to find a good approximation for *a*symmetron walls. This might be challenging if both σ and v are time-dependent. We saw in some section$^{\copyright}_{()}$ that the time-dependence of the surface tension is a game-changer, so this at least should not be neglected.

7.4 Simulative experiments within reach

- Better spatial resolution
- Look at already-formed walls, i.e. drop the formation (see if it matters for the GWs) (time-dep. tension complicates things)

Chapter 8

Conclusion and Outlook

- Surface-tension tension: There is a strong dependence on σ.
- what I would do if time
- actual observables
- concluding remarks

8.1 Applications

8.2 Future work

Bibliography

[1] Julian Adamek, David Daverio, Ruth Durrer, and Martin Kunz. Gevolution: A cosmological N-body code based on General Relativity. *Journal of Cosmology and Astroparticle Physics*, 2016(07):053–053, July 2016. ISSN 1475-7516. doi: 10.1088/1475-7516/2016/07/053. URL http://arxiv.org/abs/1604.06065.

[2] Jose J. Blanco-Pillado, Daniel Jiménez-Aguilar, Jose M. Queiruga, and Jon Urrestilla. The dynamics of Domain Wall Strings. *Journal of Cosmology and Astroparticle Physics*, 2023(05):011, May 2023. ISSN 1475-7516. doi: 10.1088/1475-7516/2023/05/011. URL http://arxiv.org/abs/2209.12945.

[3] Clare Burrage, Bradley March, and Aneesh P. Naik. Accurate computation of the screening of scalar fifth forces in galaxies. *Journal of Cosmology and Astroparticle Physics*, 2024:004, April 2024. ISSN 1475-7516. doi: 10.1088/1475-7516/2024/04/004. URL https://ui.adsabs.harvard.edu/abs/2024JCAP...04..004B.

[4] Sean M. Carroll. *Spacetime and Geometry: An Introduction to General Relativity*. Cambridge University Press, July 2019. ISBN 978-0-8053-8732-2 978-1-108-48839-6 978-1-108-77555-7.

[5] Øyvind Christiansen. *Cosmological Simulations of Phase Transitions in Screened Scalar-Tensor Gravity: Cosmic Acceleration, Topological Defects, Gravitational Waves and Relativistic Observables*. Doctoral thesis, 2024. URL https://www.duo.uio.no/handle/10852/113638.

[6] Øyvind Christiansen, Farbod Hassani, Mona Jalilvand, and David F. Mota. Asevolution: A relativistic N-body implementation of the (a)symmetron. *Journal of Cosmology and Astroparticle Physics*, 2023(05):009, May 2023. ISSN 1475-7516. doi: 10.1088/1475-7516/2023/05/009. URL https://iopscience.iop.org/article/10.1088/1475-7516/2023/05/009.

[7] M. P. Dąbrowski, J. Garecki, and D. B. Blaschke. Conformal transformations and conformal invariance in gravitation. *Annalen der Physik*, 521:13–32, February 2009. ISSN 0003-3804. doi: 10.1002/andp.2009521010510.1002/andp.200810331. URL https://ui.adsabs.harvard.edu/abs/2009AnP...521...13D.

[8] David Daverio, Mark Hindmarsh, and Neil Bevis. Latfield2: A c++ library for classical lattice field theory, January 2016. URL http://arxiv.org/abs/1508.05610.

[9] Justin Feng and Edgar Gasperín. Linearised conformal Einstein field equations. *Classical and Quantum Gravity*, 40:175001, September 2023. ISSN 0264-9381. doi: 10.1088/1361-6382/ace606. URL https://ui.adsabs.harvard.edu/abs/2023CQGra..40q5001F.

[10] Jaume Garriga and Alexander Vilenkin. Perturbations on domain walls and strings: A covariant theory. *Physical Review D*, 44:1007–1014, August 1991. ISSN 1550-79980556-2821. doi: 10.1103/PhysRevD.44.1007. URL https://ui.adsabs.harvard.edu/abs/1991PhRvD..44.1007G.

[11] Kurt Hinterbichler, Justin Khoury, Aaron Levy, and Andrew Matas. Symmetron cosmology. *Physical Review D*, 84(10):103521, November 2011. doi: 10.1103/PhysRevD.84.103521. URL https://link.aps.org/doi/10.1103/PhysRevD.84.103521.

[12] Akihiro Ishibashi and Hideki Ishihara. Equation of motion for a domain wall coupled to gravitational field. *Physical Review D*, 60(12):124016, November 1999. ISSN 0556-2821, 1089-4918. URL http://arxiv.org/abs/gr-qc/9802036.

[13] Niko Jokela, K. Kajantie, and Miika Sarkkinen. Gravitational wave memory and its tail in cosmology. *Physical Review D*, 106:064022, September 2022. ISSN 1550-79980556-2821. doi: 10.1103/PhysRevD.106.064022. URL https://ui.adsabs.harvard.edu/abs/2022PhRvD.106f4022J.

[14] Masahiro Kawasaki and Ken'ichi Saikawa. Study of gravitational radiation from cosmic domain walls. *Journal of Cosmology and Astroparticle Physics*, 2011(09):008–008, September 2011. ISSN 1475-7516. doi: 10.1088/1475-7516/2011/09/008. URL http://arxiv.org/abs/1102.5628.

[15] Claudio Llinares and Levon Pogosian. Domain walls coupled to matter: The symmetron example. *Physical Review D*, 90(12):124041, December 2014. doi: 10.1103/PhysRevD.90.124041. URL https://link.aps.org/doi/10.1103/PhysRevD.90.124041.

[16] Michele Maggiore. *Gravitational Waves. Vol. 2: Astrophysics and Cosmology*. Oxford University Press, March 2018. ISBN 978-0-19-857089-9.

[17] William H. Press, Barbara S. Ryden, and David N. Spergel. Dynamical Evolution of Domain Walls in an Expanding Universe. *The Astrophysical Journal*, 347:590, December 1989. ISSN 0004-637X. doi: 10.1086/168151. URL https://ui.adsabs.harvard.edu/abs/1989ApJ...347..590P.

[18] The Sage Developers. *SageMath, the Sage Mathematics Software System (Version 10.1)*, 2023.

[19] Tanmay Vachaspati. *Kinks and Domain Walls: An Introduction to Classical and Quantum Solitons*. Cambridge University Press, Cambridge, 2006. ISBN 978-0-521-83605-0. doi: 10.1017/CBO9780511535192. URL https://www.cambridge.org/core/books/kinks-and-domain-walls/98D525CCD885D53F51BDFC3B08A711A6.

Appendix A

Derivations

A.1 Linearised gravity

Relevant for Section 2.4

We go through the derivation of the first order tensor perturbations—the gravitational waves—on a flat FRW background. We begin with the general background metric $g_{\mu\nu}$ and look at perturbations up to second order, $\mathring{g}_{\mu\nu} = g_{\mu\nu} + \delta^{(1)}g_{\mu\nu} + \delta^{(2)}g_{\mu\nu}$

[13]

A.2 Variation of stress–energy tensor

A.3 Fourier space stress–energy tensor: sinusoidal

Relevant for ??

We look at $\mathscr{E}(y) = \sin py$ in $\epsilon = \varepsilon(\tau)\mathscr{E}(y)$

The trick is to identify the Jacobi–Anger expansion,[1]

$$\mathrm{e}^{\mathrm{i}x\sin\theta} = \sum_{n=-\infty}^{\infty} \mathsf{J}_n(x)\mathrm{e}^{\mathrm{i}n\theta}. \tag{A.1}$$

[1] The analogous relation for cosine is obtained by inserting $\theta = \theta' + \pi/2$ to get an extra factor i^n inside the sum.

Appendix B

TITLE (Stable Symmetron)

The normal picture in the expanding universe is

$$\chi_{\mathrm{dw}}(a, z - z_{\mathrm{w}}) = \chi_{\pm} \tanh\left(\frac{a\chi_{+}(z - z_{\mathrm{w}})}{2L_{\mathrm{c}}}\right) \tag{B.1}$$

- effect on σ, δ
- also initialisation of q

We can rewrite Eq. (5.5) in terms of the time coordinate $\chi_{+} = \sqrt{1-v}$,

$$\frac{\mathrm{d}^2\breve{\chi}}{\mathrm{d}\chi_{+}^2} - \frac{1}{\chi_{+}\left(1-\chi_{+}^2\right)}\frac{\mathrm{d}\breve{\chi}}{\mathrm{d}\chi_{+}} + m^2\frac{\chi_{+}^2\left(\breve{\chi}^2 - \chi_{+}^2\right)}{\left(1-\chi_{+}^2\right)^3}\breve{\chi} = 0, \tag{B.2}$$

where

$$m = \frac{2\mu}{3\mathcal{H}_{*}(1+\mathfrak{z}_{*})} = \frac{\sqrt{2}a_{*}^{3/2}}{3\xi_{*}}. \tag{B.3}$$

The idea is to use this solution as boundary conditions for χ:

$$\chi|_{z\to\pm\infty} = \pm\breve{\chi} \quad \wedge \quad \dot{\chi}|_{z\to\pm\infty} = \pm\dot{\breve{\chi}}. \tag{B.4}$$

This generally alters the blah blah [...] ⌜Maybe rest in appendix?⌟ We solve in two regimes, each solution expanded around **(I)** $\chi_{+} = 0$ and **(II)** $\chi_{+} = 1$:

$$\breve{\chi}^{(\mathrm{I})} = \chi_{*} + \frac{C}{2}\chi_{+}^2 + \frac{C - \chi_{*}^3 m^2}{8}\chi_{+}^4, \tag{B.5a}$$

$$\breve{\chi}^{(\mathrm{II})} = \chi_{+} + \frac{8(3-m^2)}{m^4}(\chi_{+}-1)^3 + \frac{1440 - 636m^2 + 41m^4}{2m^6}(\chi_{+}-1)^4. \tag{B.5b}$$

We determine χ_{*} and C by matching these expressions at $\chi_{+}^{\mathrm{match}}$, i.e. solving

$$\begin{aligned}\breve{\chi}^{(\mathrm{I})}\big|_{\chi_{+}=\chi_{+}^{\mathrm{match}}} &= \breve{\chi}^{(\mathrm{II})}\big|_{\chi_{+}=\chi_{+}^{\mathrm{match}}} \\ \frac{\mathrm{d}\breve{\chi}^{(\mathrm{I})}}{\mathrm{d}\chi_{+}}\Big|_{\chi_{+}=\chi_{+}^{\mathrm{match}}} &= \frac{\mathrm{d}\breve{\chi}^{(\mathrm{II})}}{\mathrm{d}\chi_{+}}\Big|_{\chi_{+}=\chi_{+}^{\mathrm{match}}}\end{aligned} \tag{B.6}$$

The initial conditions best suited for the smallest oscillations possible are given by

$$\breve{\chi} = \begin{cases}\breve{\chi}^{(\mathrm{I})} & \text{if } \chi_{+} \le \chi_{+}^{\mathrm{match}}, \\ \breve{\chi}^{(\mathrm{II})} & \text{if } \chi_{+} \ge \chi_{+}^{\mathrm{match}}.\end{cases} \tag{B.7}$$

Solving this for the fiducial symmetron parameters $\boldsymbol{\theta}_*^{\rm fid}$, we get $\chi_* \simeq 0.09656$, $C \simeq 5.837$ and $\chi_+^{\rm match} \simeq 0.2568$. We update the domain wall profile

$$\chi_{\rm w} = \check{\chi} \tanh\left(\frac{a\check{\chi}(z - z_{\rm w})}{2L_{\rm C}}\right) \tag{B.8}$$

and in turn the surface tension and thickness

$$\sigma_{\rm w} = \sigma_\infty \frac{1}{2}\left(3\chi_+^2 - \check{\chi}^2\right)\check{\chi} \quad \text{and} \quad a\delta_{\rm w} = \frac{\delta_\infty}{\check{\chi}}. \tag{B.9}$$

Note that both of these inngår i the thin-wall analysis in Chapter 4.

B.1 Field initialisation

- both q and χ

Appendix C

TITLE (Cylinder Functions)

The solution to

$$y'' + \frac{1-2a}{x}y' + \left[(bcx^{c-1})^2 + \frac{a^2 - \nu^2 c^2}{x^2}\right]y = 0 \tag{C.1}$$

is

$$y(x) = x^a \mathsf{Z}_\nu(bx^c), \tag{C.2}$$

where Z_ν is a linear combination of the Bessel functions of the first and second kind, J_ν and Y_ν.

Let $\nu \in \mathbb{R}$ and $n \in \mathbb{Z}$. The **Bessel** and **Neumann functions**

$$\mathsf{J}_\nu(x) =, \tag{C.3a}$$
$$\mathsf{Y}_\nu(x) = . \tag{C.3b}$$

For $\nu = n + 1/2$ we can express the functions in terms of **spherical Bessel** and **Neumann** functions

$$\mathsf{j}_n(x) = \sqrt{\frac{\pi}{2x}}\mathsf{J}_{n+1/2}(x) = +x^n\left(-\frac{1}{x}\frac{\mathrm{d}}{\mathrm{d}x}\right)^n\left(\frac{\sin x}{x}\right), \tag{C.4a}$$
$$\mathsf{y}_n(x) = \sqrt{\frac{\pi}{2x}}\mathsf{Y}_{n+1/2}(x) = -x^n\left(-\frac{1}{x}\frac{\mathrm{d}}{\mathrm{d}x}\right)^n\left(\frac{\cos x}{x}\right). \tag{C.4b}$$

These are linearly independent solutions to

$$x^2y'' + 2xy' + \Big(x^2 - n(n+1)\Big)y = 0. \tag{C.4c}$$

These are related to the **Riccati–Bessel** and **–Neumann functions** by

$$\mathsf{S}_n(x) = +x\mathsf{j}_n(x), \tag{C.5a}$$
$$\mathsf{C}_n(x) = -x\mathsf{y}_n(x), \tag{C.5b}$$

that satisfy

$$x^2y'' + \Big(x^2 - n(n+1)\Big)y = 0. \tag{C.5c}$$

Note that $\mathsf{S}_0(x) = \sin x$ and $\mathsf{C}_0(x) = \cos x$.

C.1 Properties